Conf-930164--10

RECEIVED
JUN 16 1993
OSTI

EVALUATION OF THE INTERFACIAL MECHANICAL PROPERTIES IN FIBER-REINFORCED CERAMIC COMPOSITES*

M. K. Ferber, A. A. Wereszczak, L. Riester, and R. A. Lowden
Oak Ridge National Laboratory, Oak Ridge, TN 37831

K. K. Chawla
New Mexico Tech., Socorro, NM 87801

ABSTRACT

The present study examined the application of a micro-indentation technique to the measurement of interfacial mechanical properties in fiber reinforced ceramic composites. Specific fiber/matrix systems included SiC/glass, SiC/macro-defect-free (MDF) cement, SiC/SiC, and mullite/glass. The effect of fiber coatings upon the interfacial properties was also investigated. These properties, which included the debond strength, interfacial shear stress, and residual axial fiber stress, were evaluated by measuring the force-displacement curves generated during load-unload cycles. Estimates of these three stress values were obtained by matching the experimental force-displacement curves with data predicted from an existing model.

In general the SiC/glass composites exhibited the lowest values of the interfacial shear and debond stresses. The sliding characteristics of the SiC/MDF cement and SiC/SiC composites were strongly influenced by the residual axial stress and the nature of the fiber coating. In the case of the mullite/glass composite, the high values of the interfacial shear and debond stresses reduced the measurement sensitivity, thereby increasing the uncertainty in the estimates of the interfacial properties.

---

* Research sponsored by the Department of Energy, Assistant Secretary for Conservation and Renewable Energy, Office of Transportation Technologies, as part of the High Temperature Materials Laboratory User Program, under contract DE-AC05-84OR21400 with Martin Marietta Energy Systems, Inc.

INTRODUCTION

Future energy-efficient heat engines will utilize high-performance structural materials in selected elevated-temperature areas. While monolithic ceramics such as silicon carbide and silicon nitride have been cited as excellent candidate materials for these applications, their inherent brittleness has limited their utilization as structural components. One promising solution involves the use of continuous fiber ceramic composites (CFCCs). Because these composite materials are significantly tougher than their monolithic counterparts, high-temperature structural components which are fabricated from ceramic composites should be more damage tolerant.

The optimization of the mechanical performance of CFCCs for specific high-temperature applications requires knowledge of both the constituent and interfacial (micro-mechanical) properties. For example, high toughness is generally associated with concurrently active fiber bridging and fiber pull-out processes. To maximize the bridging contribution, debonding must occur before fiber fracture as a macroscopic crack approaches a fiber. This condition is maintained as long as the ratio of the fiber strength to the interfacial shear strength, S_f/τ_s, exceeds a critical value which is determined by the fiber volume fraction, the shear transfer length, and fiber/matrix elastic properties.[1] A second condition required to maximize the toughness is that once the fiber has debonded, the matrix must remain in contact with the fiber. This will occur as long as the ratio of the residual interfacial clamping (radial) stress to the interfacial shear strength, σ^R_{ir}/τ_s, exceeds a critical value which again is a function of the fiber volume fraction and fiber/matrix elastic properties.[1]

The increment of toughening, ΔJ, arising from fiber pull-out and fiber bridging will also be dependent upon the interfacial properties. Analyses have shown that ΔJ (pull-out) $\propto (\mu\, \sigma^R_{mz})$ and ΔJ (bridging) $\propto 1/(\mu^2\, \sigma^R_{mz})$, where μ is the coefficient of friction and σ^R_{mz} is the residual axial stress in the matrix.[2] This latter parameter can be related to the residual axial stress in the fiber, σ^R_{fz}. Maximum toughening is expected when an optimum comprimise between these parameters is achieved.

The first matrix cracking stress, σ_{mu}, is another macroscopic property which is strongly dependent upon interfacial characteristics. For the case of a simple unidirectional fiber-reinforced composite, σ_{mu} is given by,

$$\sigma_{mu}/E_c = \{[12\, \tau_i\, \gamma_m\, V_f^2\, E_f\,]/[r\, V_m\, E_c\, E_m^2]\}^{1/3} \qquad (1a)$$

where

$$E_c = (V_f\, E_f + V_m\, E_m), \qquad (1b)$$

τ_i is the interfacial sliding shear stress, γ_m is the fracture energy of the matrix, E is the elastic modulus, V is the volume fraction, and r is the fiber radius.[3] The subscripts c, m, and f refer to the composite, matrix, and

fiber, respectively. Equation 1 is valid when the residual axial stresses are zero. For a nonzero value of σ^R_{mz}, σ_{mu} is given by[3]

$$\sigma_{mu}/E_c + \sigma^R_{mz}/E_m = \{[12\ \tau_i\ \gamma_m\ V_f^2\ E_f\ ]/[r\ V_m\ E_c\ E_m^2]\}^{1/3}. \qquad (2)$$

Because of the importance of interfacial properties in controlling the mechanical response of CFCCs, considerable effort has been directed towards the development of experimental techniques and mathematical expressions required to estimate these properties from fiber sliding experiments. One commonly applied technique involves displacing individual fibers with a micro-indenter or mechanical properties microprobe (MPM) equipped with both load and displacement sensors.[4,5]

Figure 1 provides a schematic representation of the stress-displacement characteristics of a fiber loaded with the MPM. Because the sliding length in such a test is generally much smaller than the overall specimen thickness, the fiber is pushed into the matrix but not through it (i.e., a fiber push-in test). The debond stress, σ_d, is the stress at which sliding initiates and is a function of the interfacial shear strength, τ_s. The shape of the loading curve depends upon μ, σ^R_{ir}, σ^R_{fz},* and the elastic properties of both the matrix and fiber. During unloading, the extent of fiber recovery as characterized by the ratio, u_o/u_{max}, depends strongly upon the values of σ^R_{fz} and the Poisson's ratio of the fiber, ν_f. When σ^R_{fz} and ν_f are zero, u_o/u_{max} will be 0.5 (Ref. 5). However, as either σ^R_{fz} or ν_f become more positive, u_o/u_{max} decreases accordingly.

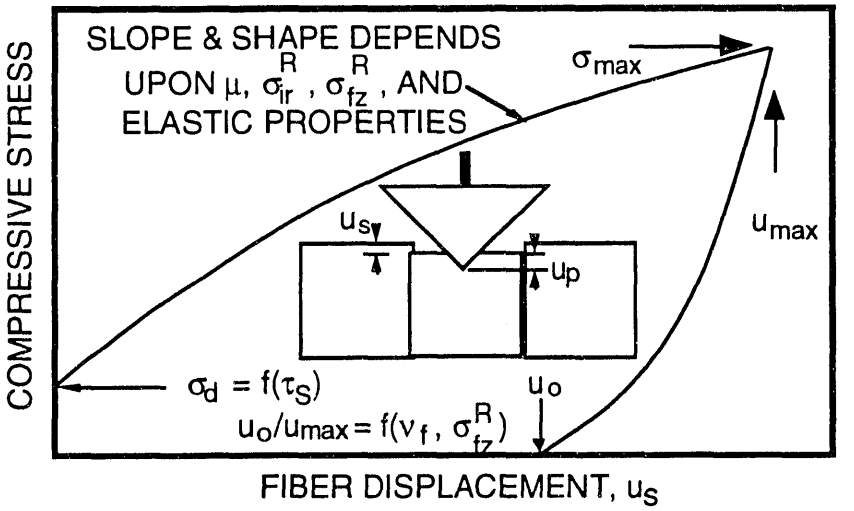

Figure 1. Schematic Representation of the Stress-Displacement Characteristics Obtained from Indentation Push-In Test.

---

* Unless otherwise stated, positive values of σ^R_{ir}, σ^R_{fz}, and σ_d denote compressive stresses.

Numerous models have been developed to describe the stress-displacement curves like the one in Fig. 1 in terms of the interfacial properties.[4-10] For example, Marshall and Oliver[5] specifically addressed the effects of the residual axial stress, σ^R_{fz}, upon the shape stress-displacement (σ-u_s) curves generated during loading/unloading. While their model also accounted for fiber debonding, it neglected the effects of the Poisson's expansion of the fiber during loading. These Poisson's ratio effects were considered in an early model by Hsueh[6] by including a term for the interfacial clamping stress induced from the Poisson's expansion of the fiber, σ_{ir}, in the expression,

$$\tau_i = \mu\,(\sigma^R_{ir} + \sigma_{ir}). \qquad (3)$$

Variations of σ_{ir} along the sliding length result in similar variations in τ_i. Two limitations of his model were that it (1) required an iterative numerical solution for the fiber sliding length and (2) did not account for the effects of either residual axial or debond stresses upon the σ-u_s behavior. Both limitations have been addressed in a more recent model which simplifies the calculation of the interfacial properties by averaging the Poisson's ratio effects over the sliding length.[7]

The present study summarizes results of recent fiber sliding studies involving SiC/glass, SiC/macro-defect-free (MDF) cement, SiC/SiC, and mullite/glass composites. The motivation of these studies was to examine the application of both the micro-indentation push-in technique and the associated mathematical models to the measurement of interfacial mechanical properties. The effect of fiber coatings upon the interfacial properties was also investigated. Estimates of debond stress, interfacial sliding shear stress, and residual axial fiber stress were obtained by first measuring the force-displacement curves and then matching these curves with data predicted from existing models.

EXPERIMENTAL PROCEDURE

Table 1 summarizes the composite systems examined in the embedded in an 31.8 mm (1.25") diameter plastic mount such that the fibers were perpendicular to the mount surface. This surface was subsequently ground and polished to a 0.25 μm finish using standard ceramographic techniques.

For each of the composite systems listed in Table 1, a minimum of 5 fibers was loaded using a commercial MPM.* The MPM used in the present study is capable of accurately applying mN loads via a Berkovich pyramidal diamond indenter having the same depth-area ratio as a Vickers diamond tip indenter. The fiber loading history involved an application of a predetermined constant loading rate to a maximum force followed by a constant unloading rate until 95% of the force was

---

* Nano Instruments Inc., Knoxville, TN.

removed. This sequence was followed first by a hold segment, necessary for correction of thermal drift, and then by complete unloading. The magnitudes of the force and displacement were continuously measured during each segment of the loading procedure with resolutions of 2.4 μN and 0.4 nm, respectively. The maximum load capability of the instrument was 0.12 N.

Table 1. Summary of Composite Systems Utilized in Interfacial Properties Study.

Fiber	Matrix	Coating	Processing	Ref.
SiC*	LAS Glass**	None	Hot Pressed	11
SiC*	MDF Cement	Stearic Acid Silane	Warm Pressed	12,13
SiC*	SiC	Graphite	CVI	14
Mullite***	Glass	BN	Hot Pressed	15

* Nicalon fiber, Nippon Carbon Company, Tokyo, Japan.
**Li_2O-Al_2O_3-SiO_2 Glass.
*** Nextel 480, 3M Company, Minneapolis, Minnesota.

In order to generate fiber displacement, u_s, versus stress, σ, curves from the MPM data, the indenter penetration into the fiber, u_p, was first subtracted from the total displacement of the indenter ($u_p + u_s$). The relationship between stress and u_p was determined by applying the loading procedure to relatively large fibers which did not slide. In order to facilitate the subtraction of u_p from the total displacement versus stress curves, the stress dependence of u_p was represented by two curve fitted polynomial expressions each describing the loading and unloading curves, respectively.

RESULTS AND DISCUSSION

Figure 2 illustrates the σ-u_s data obtained for the SiC/LAS composite. The predicted curve in this figure was calculated using the early model by Hsueh.[6] In this case, the Poisson's expansion of the fiber is used to account for the deviation of the experimental u_o/u_{max} ratio (= 0.35) from the value of 0.5 obtained for $v_f = 0$. The agreement between the predicted and experimental curves is quite good. The sliding resistance for this composite is characterized by the parameters μ (= 0.09) and σ^R_{ir} (= 21 MPa) instead of τ_i, which varies along the sliding length in accordance with Eq. 3.

A key limitation of the predicted curve in Fig. 2, is that it neglects the effect of the residual axial stress in the fiber, σ^R_{fz}. As discussed above, when σ^R_{fz} is compressive, the relative fiber recovery during unloading will increase such that u_o/u_{max} decreases. One method for distinguishing between the effects of σ^R_{fz} and v_f involves measuring u_o/u_{max} as a function of the peak stress (σ_{max} in Fig. 1).[16] As shown in Fig. 3, the

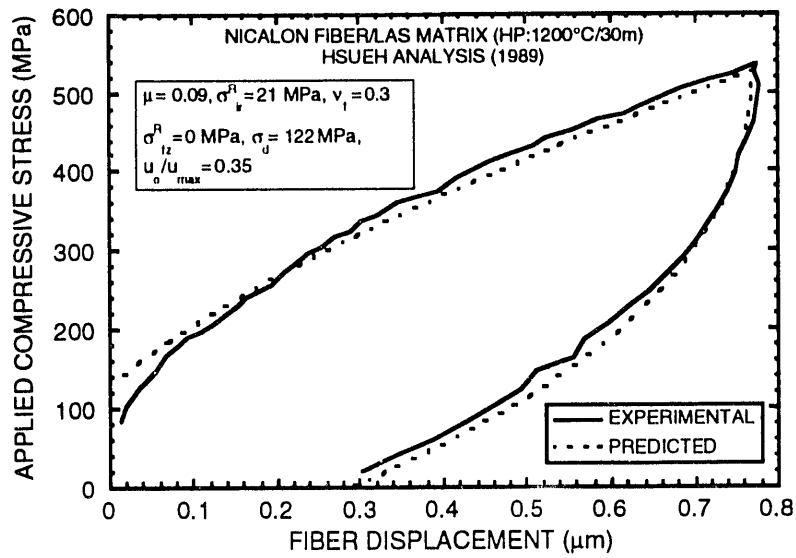

Figure 2. Typical Stress-Fiber Displacement Curve for the SiC/LAS Glass Composite.

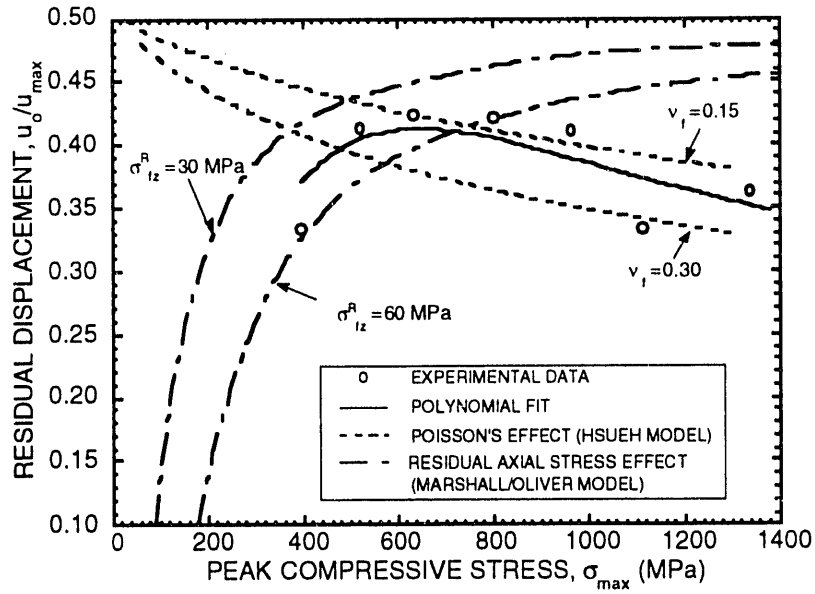

Figure 3. Effect of Peak Stress Upon the Relative Displacement Ratio for the SiC/LAS Glass Composite. Experimental data are compared with predictions based on the analyses of Hsueh and Marshall/Oliver.

experimental values of u_o/u_{max} exhibit a maximum as σ_{max} is increased. This trend is quite consistent with the predicted curve based on the analyses of Hsueh[6] and Marshall/Oliver.[5] The former analysis, which accounts for Poisson's effects only, was conducted for $\mu = 0.09$ and $\sigma^R_{ir} =$ -21 MPa for $\nu_f = 0.3$ and $\nu_f = 0.15$. The Marshall/Oliver model, which ignores Poisson's effects, was used to predict the effect of σ^R_{fz} upon the peak stress dependence of the relative residual displacement for both $\sigma^R_{fz} = 30$ MPa and $\sigma^R_{fz} = 60$ MPa. The choice of these two σ^R_{fz} values was based upon the application of the Marshall model to the description of the experimental applied stress versus displacement data for the SiC/LAS composite.

The predicted curves in Fig. 3 reveal opposing trends in the effects of Poisson's ratio and residual axial stress upon the peak stress dependence of u_o/u_{max}. Considering the curves generated for $\sigma^R_{fz} =$ 60 MPa (Marshall model) and $\nu_f = 0.15$ (Hsueh model), it is evident that for $\sigma_{max} < 650$ MPa, the residual axial stress dominates the relative residual displacement as reflected by the large deviation of the predicted u_o/u_{max} from the value of 0.5 which would result for $\nu_f = 0$ and $\sigma^R_{fz} =$ 0 MPa. As σ_{max} exceeds 650 MPa, u_o/u_{max} is controlled by the Poisson's ratio effect. A similar opposing trend is exhibited by the experimental data, which are well-described by the Marshall model for $\sigma_{max} < 650$ MPa and the Hsueh model for $\sigma_{max} > 650$ MPa. The predicted curves in Fig. 3 also illustrate the effects of the magnitudes σ^R_{fz} and ν_f upon the relative recovery during fiber sliding. In the case of the Marshall model, a small decrease in σ^R_{fz} shifts the σ_{max} versus u_o/u_{max} curve to the left thereby lowering the critical transition stress from 650 MPa to 420 MPa. In the Hsueh model, an increase in ν_f increases the extent of the Poisson's ratio effect. The transition stress is again lowered to approximately 550 MPa.

The residual axial stress in the fiber plays an even more important role in the SiC/MDF cement composite. Using the Marshall/Oliver analysis, σ^R_{fz} is estimated to be 66 and 129 MPa for the stearic acid and silane coated fibers, respectively (Figs. 4a and b). For the latter specimen, the fiber recovery upon unloading is greater than the displacement during loading ($u_o/u_{max} = -0.31$). Based on an analysis similar to that used in Fig. 3, Poisson's ratio effects are expected to be negligible.[10]

A typical stress-displacement curve for the mullite/glass composite is shown in Fig. 5. Even with the 0.2 μm BN coating, sliding in this system was quite limited as evidenced by a relatively high value of τ_i (65 MPa). When no coating was present, sliding could not be measured. This difference in sliding characteristics is consistent with previous studies which showed a marked improvement in mechanical performance when the BN coating was applied to the fibers.[15]

The utilization of the interfacial properties in the calculation of the macro-mechanical behavior of the SiC/SiC composite is illustrated in Fig 6. The interfacial sliding shear stress for this system ($\tau_i = 25$ MPa)

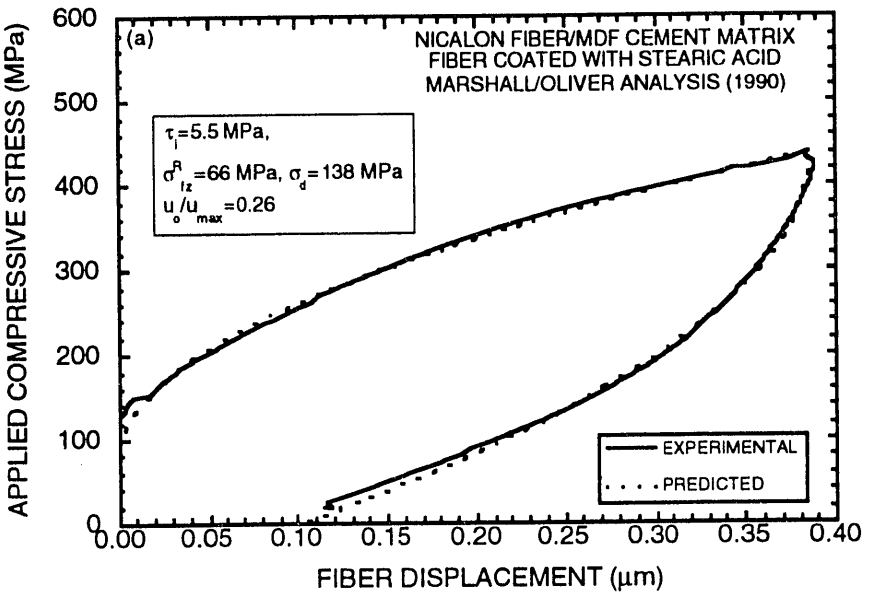

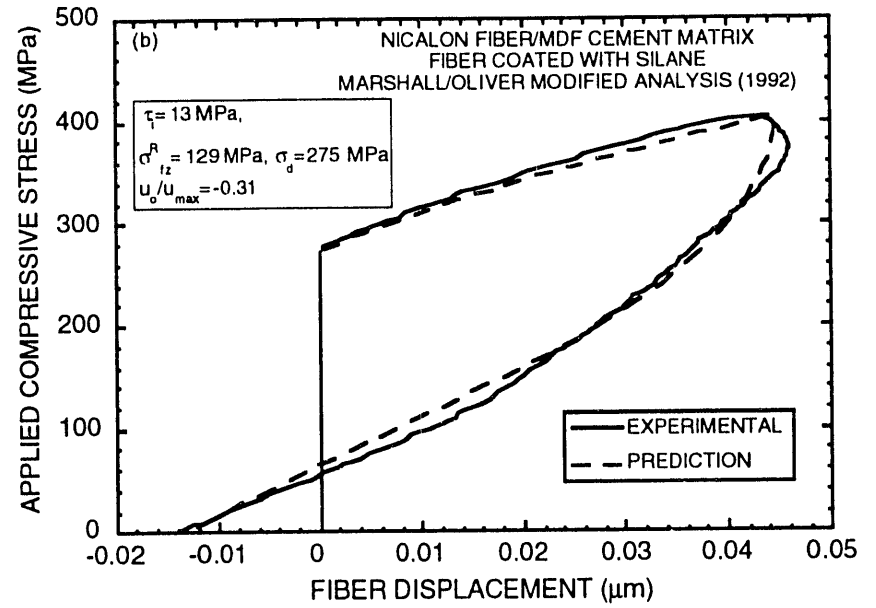

Figure 4. Stress-Fiber Displacement Curves for the SiC/MDF Cement Composite: (a) Fibers Coated with Stearic Acid and (b) Fibers Coated with Silane.

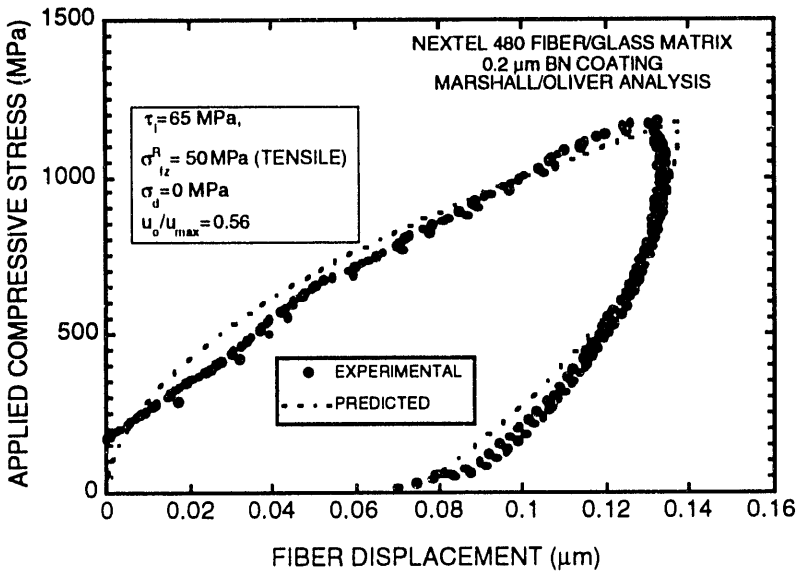

Figure 5. Typical Stress-Fiber Displacernent Curve for the Mullite/Glass Glass Composite.

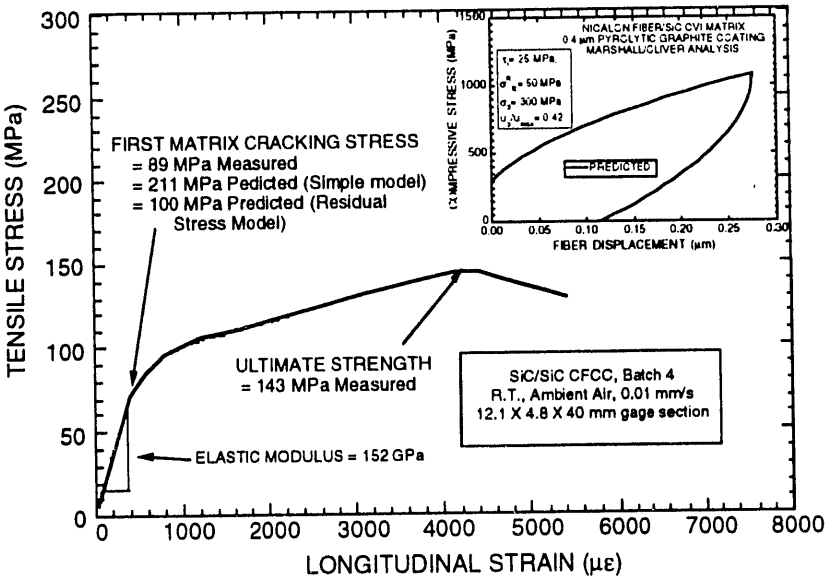

Figure 6. Comparison of Experimentally-Measured and Predicted Values of the First Matrix Cracking Stress in the SiC/SiC Composite.

was used in conjunction with Eqs. 1 and 2 to estimate the first matrix cracking stress. Values for the other parameters were as follows: r = 8.5 μm, E_f = 150 GPa, E_m = 350 GPa, γ_m = 15 J/m^2, and V_f = 0.41. Using equations given in Ref. 17 in conjunction with the predicted value of σ^R_{fz} (= 50 MPa), the residual axial stress in the matrix was estimated to be 35 MPa (tensile). As indicated in Fig. 6, reasonable agreement between experimental and predicted values of σ_{mu} could only be obtained if the residual axial stress in the matrix was included in the analysis (Eq. 1b). The fact that the predicted value of 100 MPa exceeds the experimental value of 89 MPa may be a result of neglecting the effects of fiber debonding in the calculation of σ_{mu}.

CONCLUSIONS

The push-in studies involving the MPM provided reasonable measurements of fiber sliding for those systems in which both the fiber diameters were small (<25 μm diameter) and the values of τ_i and σ_d were low (τ_i < 50 MPa and σ_d < 0.5 σ_{max}). When these conditions were not met as in the case of the mullite/glass composites, the uncertainty in the polynomial fits used to describe the σ-u_p relationship constituted a major source of error in the estimates of the interfacial properties. The reduction of this error would have required the use of either higher peak loads or a small flat-bottomed indenter probe to eliminate the contribution of u_p to the overall sliding.

The data generated for the SiC/LAS and SiC/MDF composites indicated that both Poisson's ratio and the residual axial stress in the fiber could have a significant effect upon the sliding characteristics. The relative contribution of each of these parameters could be determined by measuring the relative residual displacement as a function of the peak stress. In particular, below a critical peak stress, u_o/u_{max} was primarily a function of σ^R_{fz} with u_o/u_{max} decreasing as the peak stress decreased. Above the critical peak stress, Poisson's expansion of the fiber controlled the value of u_o/u_{max} with u_o/u_{max} decreasing as the peak stress increased.

Although the models examined in this study provided good descriptions of the stress-displacement characteristics associated with the various composite systems, additional model refinements will be required for the analysis of real composite systems. For example, attention must be given to the treatment of more complex fiber architectures. These models must also account for anisotropy of the elastic properties. Finally, the shear-lag analysis, which is fundamental to most of the existing models, must be extended to three component systems involving fiber, coating, and matrix.

REFERENCES

(1) Chun-Hway Hsueh, "Requirements of Frictional Debonding at Fiber/Matric Interfaces for Tough Ceramic Composites," *Composites Eng.*, **2** [8] 655-63 (1992).

(2) B. B. Marshall and A. G. Evans, "The Influence of Residual Stress on the Toughness of Reinforced Brittle Materials," *Mater. Forum*, **11**, 304-12 (1988).

(3) B. Budiansky, J. W. Hutchinson, and A.G. Evans, "Matrix Fracture in Fibre-Reinforced Ceramics," *J. Mech. Phys. Solids*, **34** [2] 167-189 (1986).

(4) D. B. Marshall and W. C. Oliver, "Measurement of Interfacial Mechanical Properties in Fiber-Reinforced Ceramic Composites," *J. Am. Cer. Soc.*, **70** [8] 542-548 (1987).

(5) D. B. Marshall and W. C. Oliver, "An Indentation Method for Measuring Residual Stresses in Fiber Reinforced Ceramics," *Mat. Sci. Eng.* , **A126**, 95-103 (1990).

(6) C. H. Hsueh, M. K. Ferber, and P. F. Becher, "Stress-Displacement Relation of Fiber for Fiber-Reinforced Ceramic Composites During (Indentation) Loading and Unloading," *J. Mater. Res.*, **4** [6] 1529-37 (1989).

(7) C. H. Hsueh, "Evaluations of Interfacial Properties of Fiber-Reinforced Ceramic Composites using Mechanical Properties Microprobe," in review, Journal of the American Ceramic Society.

(8) R. J. Kerans and T. A. Parthasarathy, "Theoretical Analysis of the Fiber Pullout and Pushout Tests," *J. Am. Cer. Soc.*, **74** [7] 1585-96 (1991).

(9) D. B. Marshall, "Analysis of Fiber Debonding and Sliding Experiments in Brittle Matrix Composites," *Act Metall. Mater*, **40** [3] 427-41 (1992).

(10) C. H. Hsueh and M. K. Ferber, "Evaluations of Residual Axial Stresses and Interfacial Friction in Nicalon Fiber-Reinforced Macro-Defect-Free Cement Composites," in press, Journal of Materials Science.

(11) J. R. VanValzah, "Processing, Interfacial Characterization, and Mechanical Property Evaluation of SiC Fiber/Li_2O-Al_2O_3-SiO_2 Glass Matrix Composites," M.S. Thesis, Univ. of Illinois, Urbana, IL, 1986.

(12) M. K. Ferber, A. A. Wereszczak, D. Hansen, and J. Homeny, "Evaluation of the Interfacial Mechanical Properties in SiC Fiber-Reinforced MDF Cement Composites, " in press, Composite Science and Technology.

(13) D. H. Hansen, "Interfacial Characterization of SiC Fiber/MDF Matrix Composites," M.S. Thesis, Univ. of Illinois, Urbana, IL, 1990.

(14) M. J. Jenkins and M. K. Ferber, unpublished work, Oak Ridge National Laboratory, May 1992.

(15) R. U. Vaidya, J. Fernando, K. K. Chawla, and M. K. Ferber, "Effect of Fiber Coating on the Mechanical Properties of a Nextel 480 Fiber Reinforced Glass Matrix Composite, " *Matl. Sci. and Eng.* **A150**, 161-9 (1992).

(16) C. H. Hsueh, M. K. Ferber, and A. A. Wereszczak, "The Relative Residual Fiber Displacement after Indentation Loading and Unloading of Fiber-Reinforced Ceramic Composites, " in publication, Journal of Material Science.

(17) Chun-Hway Hsueh, Paul F. Becher, and Peter Angelini, "Effects of Interfacial Films on Thermal Stresses in Whisker-Reinforced Ceramics," *J. Am. Cer. Soc.*, **71** [11] 929-33 (1988).

EVALUATION OF THE INTERFACIAL MECHANICAL PROPERTIES IN FIBER-REINFORCED CERAMIC COMPOSITES

M. K. Ferber, A. A. Wereszczak, L. Riester, and R. A. Lowden
Oak Ridge National Laboratory
Oak Ridge, TN

K. K. Chawla
New Mexico Tech.
Socorro, NM

17th Annual Conference on Composites
and Advanced Ceramics
January, 14, 1993
Cocoa Beach, Florida

*Research sponsored by the U. S. Department of Energy, Assistant Secretary for Conservation and Renewable Energy, Office of Transportation Technologies, as part of the High Temperature Materials Laboratory User Program, under contract DE-AC05-84OR21400 with Martin Marietta Energy Systems, Inc.

PRESENT CFCC SUPPORTED PROGRAM ON INTERFACE STUDIES HAS SEVERAL OBJECTIVES

- MEASUREMENT OF INTERFACIAL PROPERTIES
  - EXAMPLES INCLUDE INTERFACIAL SHEAR STRENGTH, SLIDING SHEAR STRESS, AND RESIDUAL AXIAL STRESS
  - FURTHER DEVELOPMENT OF TEST INSTRUMENTATION AND METHODOLOGY
  - INDENTATION PUSH-IN AND PUSH-THROUGH TESTS ARE SPECIFICALLY ADDRESSED

- MODELLING OF FIBER DEBONDING AND SLIDING UNDER POINT LOADING
  - RELATE STRESS-DISPLACEMENT CURVES TO INTERFACIAL PROPERTIES

- RELATE INTERFACIAL PROPERTIES TO MACRO-MECHANICAL BEHAVIOR
  - REQUIRES APPLICATION OF EXISTING MODELS FOR TOUGHENING AND MATRIX CRACKING
  - USE RESULTS TO THE OPTIMIZE FIBER-MATRIX INTERFACES

PRESENTATION WILL COVER FOUR ASPECTS OF INTERFACIAL BEHAVIOR

- MOTIVATION FOR MEASUREMENT OF INTERFACIAL PROPERTIES
  - RELATIONSHIP TO COMPOSITE MECHANICAL PROPERTIES
- EXPERIMENTAL INDENTATION TECHNIQUES USED TO MEASURE INTERFACIAL PROPERTIES
  - COMMONLY USED LOADING CONFIGURATIONS
  - CURRENT INSTRUMENTATION FOR PUSH-IN TESTING
- MODELLING OF STRESS-DISPLACEMENT CURVES ASSOCIATED WITH FIBER SLIDING MEASUREMENTS
  - REVIEW OF EXISTING MODELS
  - REQUIRED MODEL REFINEMENTS
- CASE HISTORIES

A NUMBER OF IMPORTANT PHYSICAL PROPERTIES ARE ASSOCIATED WITH THE FIBER/MATRIX INTERFACE

- INTERFACIAL SHEAR STRENGTH (τ_S) OR FRACTURE ENERGY
  - RELATED TO INTERFACIAL DEBOND STRESS (σ_d)
  - DETERMINED BY THE EXTENT OF CHEMICAL BONDING AND SURFACE ROUGHNESS

- INTERFACIAL SLIDING SHEAR STRESS (τ_i)
  - MAY BE ASSOCIATED WITH FRICTIONAL OR SURFACE ROUGHNESS EFFECTS
  - FOR COULOMBIC FRICTIONAL INTERFACES, THE COEFFICIENT OF FRICTION (μ) AND RESIDUAL NORMAL (RADIAL) STRESSES (σ_{ir}^R) ARE CONTROLLING PARAMETERS
  - POISSON'S EXPANSION/CONTRACTION OF THE FIBER WILL GENERATE AN ADDITIONAL RADIAL STRESS COMPONENT

- RESIDUAL STRESSES
  - RADIAL STRESS INFLUENCES FRICTIONAL SLIDING
  - AXIAL STRESSES IN THE FIBER (σ_{iz}^R) ALTER THE SHEAR STRESS REQUIRED FOR DEBONDING AS WELL AS THE MAGNITUDE OF THE POISSON'S EXPANSION/CONTRACTION

OPTIMIZATION OF THE TOUGHNESS OF A COMPOSITE SYSTEM REQUIRES KNOWLEDGE OF THE INTERFACIAL PROPERTIES

- HIGH TOUGHNESS IS GENERALLY ASSOCIATED WITH FIBER BRIDGING AND FIBER PULL-OUT PROCESSES
  - AS CRACK APPROACHES THE FIBER, DEBONDING MUST OCCUR BEFORE FIBER FRACTURE

$$S_f / \tau_S > C_0(\nu_f, \nu_m, E_f, E_m, t, V_f)$$

S_f = FIBER FRACTURE STRENGTH
ν = POISSON'S RATIO
E = ELASTIC MODULUS
t = SHEAR TRANFER LENGTH
V_f = FIBER VOLUME FRACTION

  - ONCE THE FIBER HAS DEBONDED, THE MATRIX MUST REMAIN IN CONTACT WITH THE FIBER

$$-\sigma_{ir}^R / \tau_S > C_1(\nu_f, \nu_m, E_f, E_m, V_f)$$

σ_{ir}^R = RADIAL CLAMPING STRESS ON FIBER (RESIDUAL STRESS)

τ_S WILL BE A FUNCTION OF RESIDUAL AXIAL STRESS

CONDITIONS ASSOCIATED WITH INTERFACIAL DEBONDING ARE DICTATED BY THE b/a RATIO

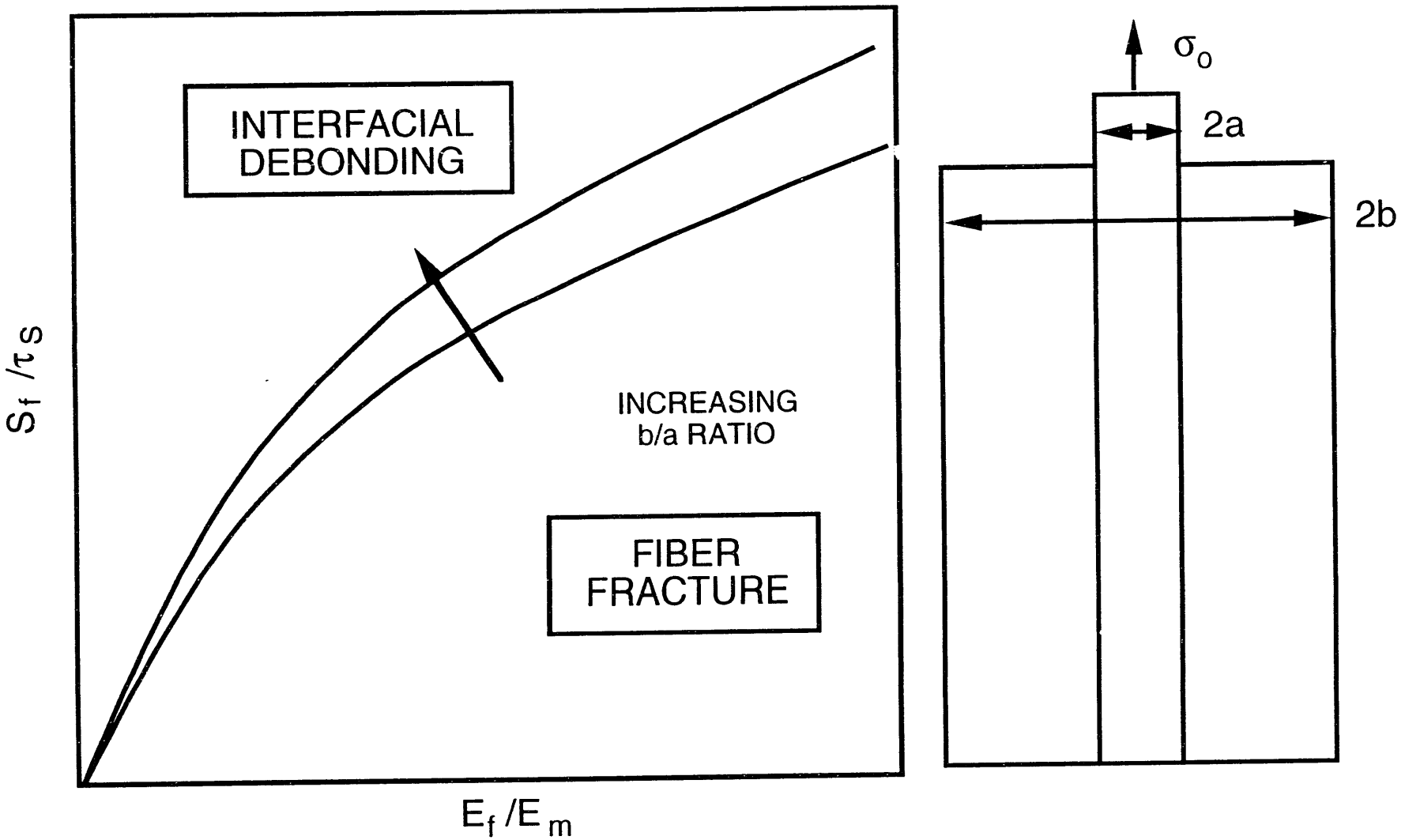

THE POISSON'S RATIO OF THE FIBER INFLUENCES THE CONDITIONS REQUIRED FOR FRICTIONAL DEBONDING

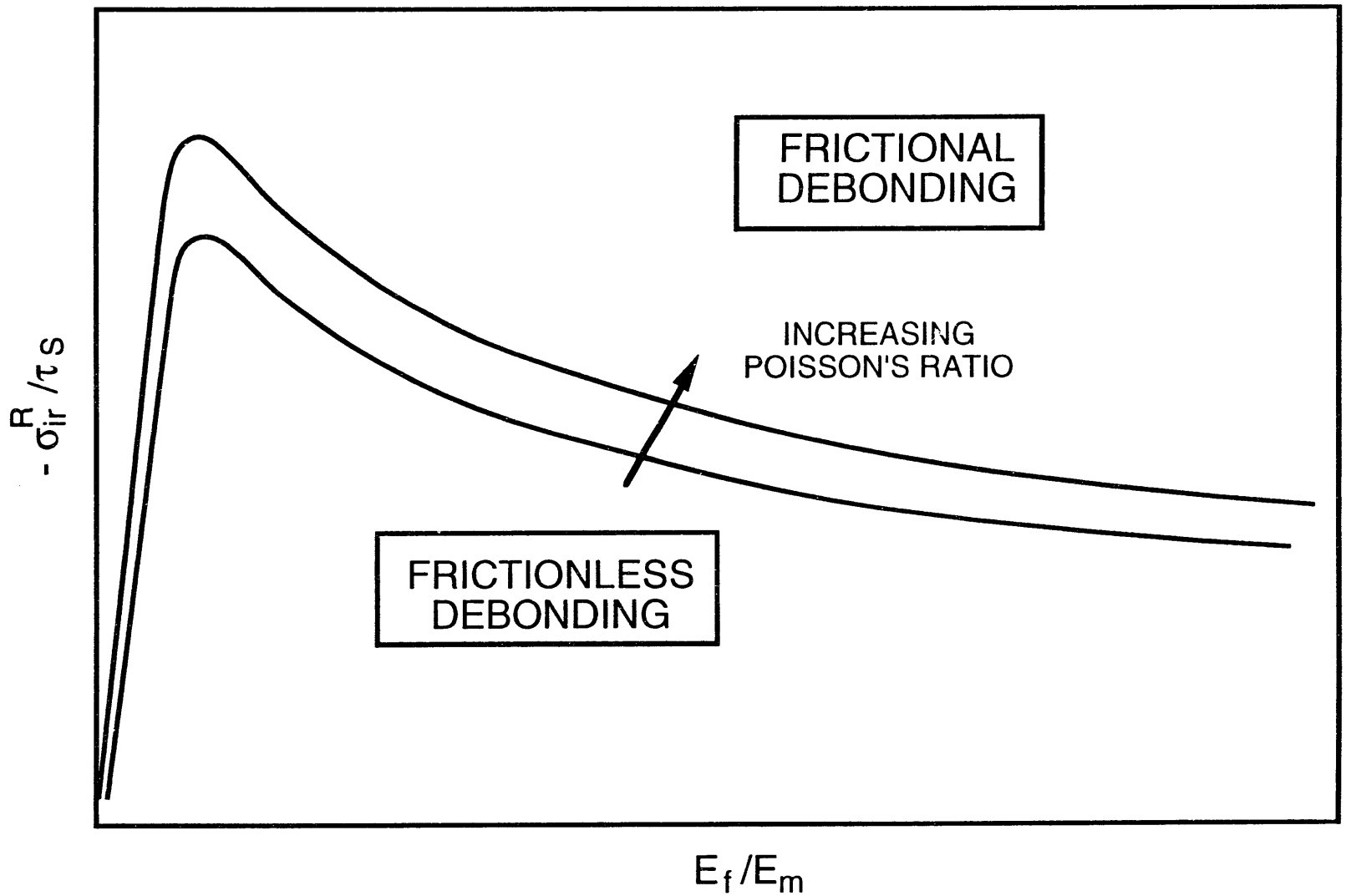

TOUGHENING INCREMENT (ΔJ) ARISING FROM FIBER BRIDGING AND PULL-OUT IS ALSO A FUNCTION OF INTERFACIAL PROPERTIES

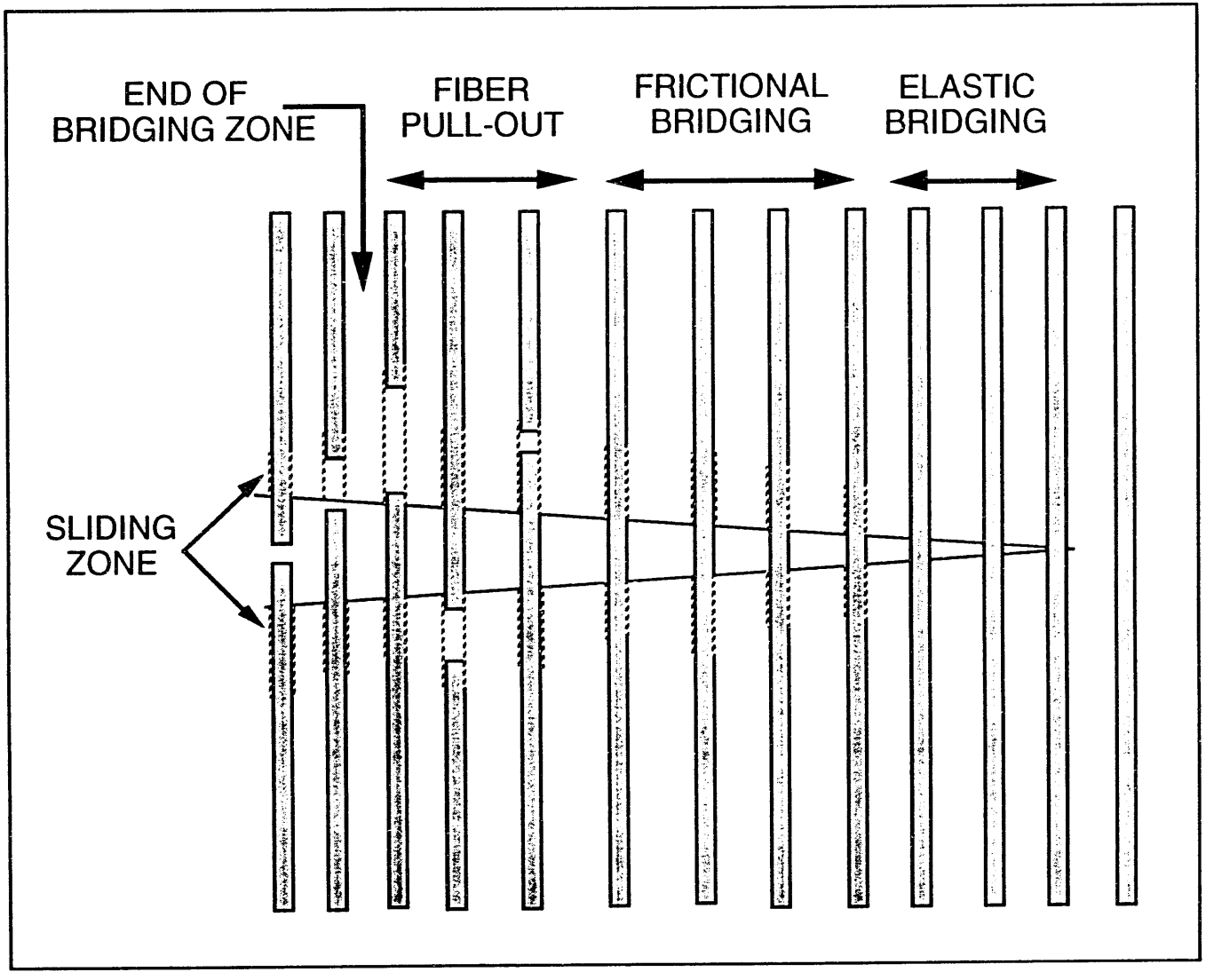

FIBER PULL-OUT

$$\Delta J \propto \mu \sigma_{mz}^{R}$$

FRICTIONAL BRIDGING

$$\Delta J \propto 1/(\mu^{2} \sigma_{mz}^{R})$$

THREE LOADING GEOMETRIES ARE COMMONLY USED TO EVALUATE INTERFACIAL PROPERTIES

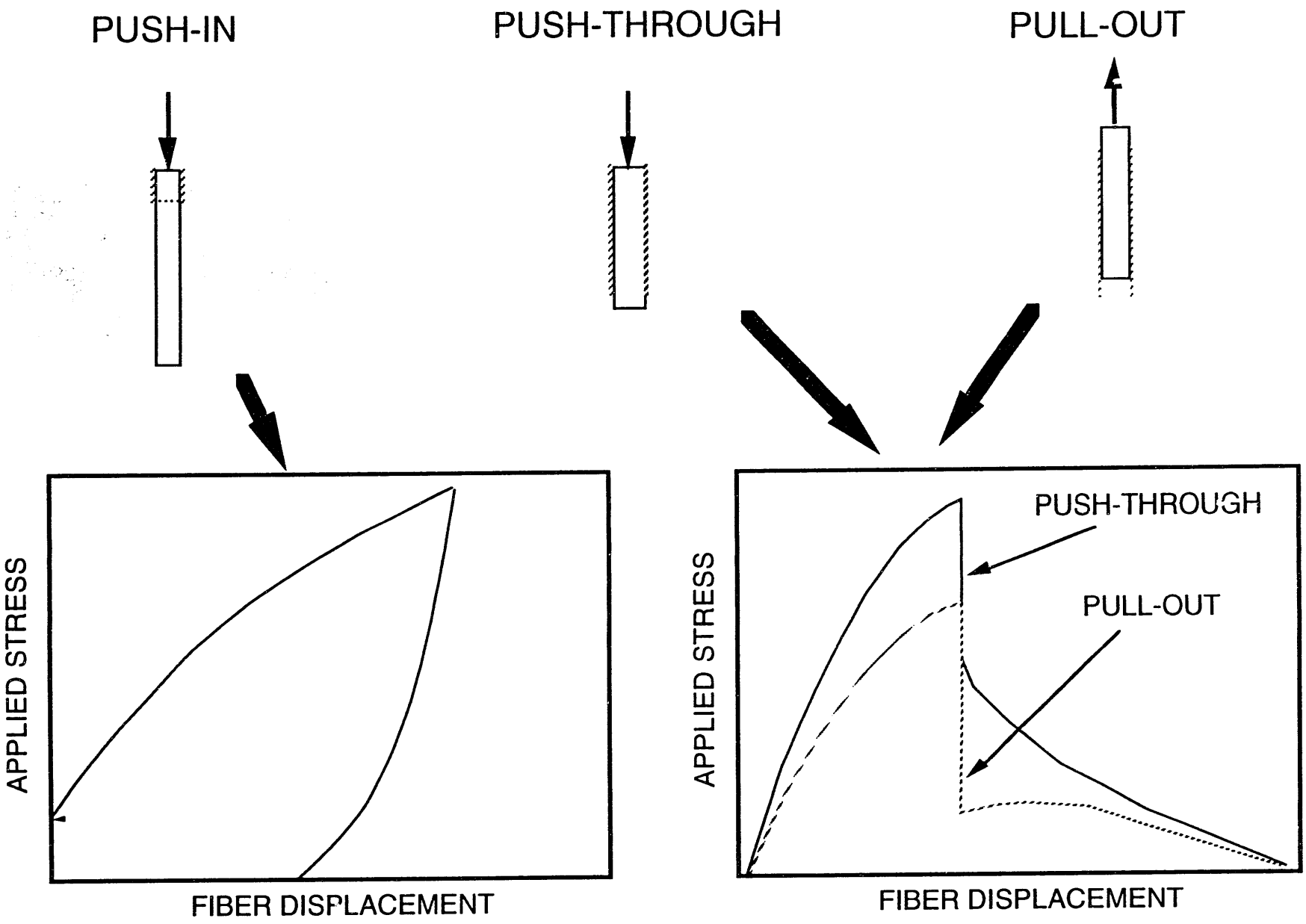

SEVERAL ADVANTAGES AND DISADVANTAGES ARE ASSOCIATED WITH THE APPLICATION OF PUSH-IN TECHNIQUES

- ADVANTAGES
  - INTERFACIAL PROPERTIES CAN BE DETERMINED FROM TESTS ON A SINGLE FIBER
  - SPECIMEN PREPARATION IS RELATIVELY SIMPLE
  - COMMERCIAL MACHINES ARE NOW EQUIPPED WITH HIGHLY SENSITIVE DISPLACEMENT MEASUREMENT DEVICES

- DISADVANTAGES
  - LOAD LIMITATIONS RESTRICT TEST TO SMALL DIAMETER FIBERS
  - PENETRATION OF FIBER BY PROBE LIMITS ULTIMATE SENSITIVITY OF THE TECHNIQUE
  - SLIDING LENGTH LIMITED BY INDENTER SHAPE

INSTRUMENTATION TYPICALLY INVOLVES USE OF A NANOINDENTER OR MECHANICAL PROPERTIES MICROPROBE

NANOINDENTER IS WELL-SUITED TO THE MEASUREMENT OF SLIDING DISPLACEMENTS IN SMALL FIBERS

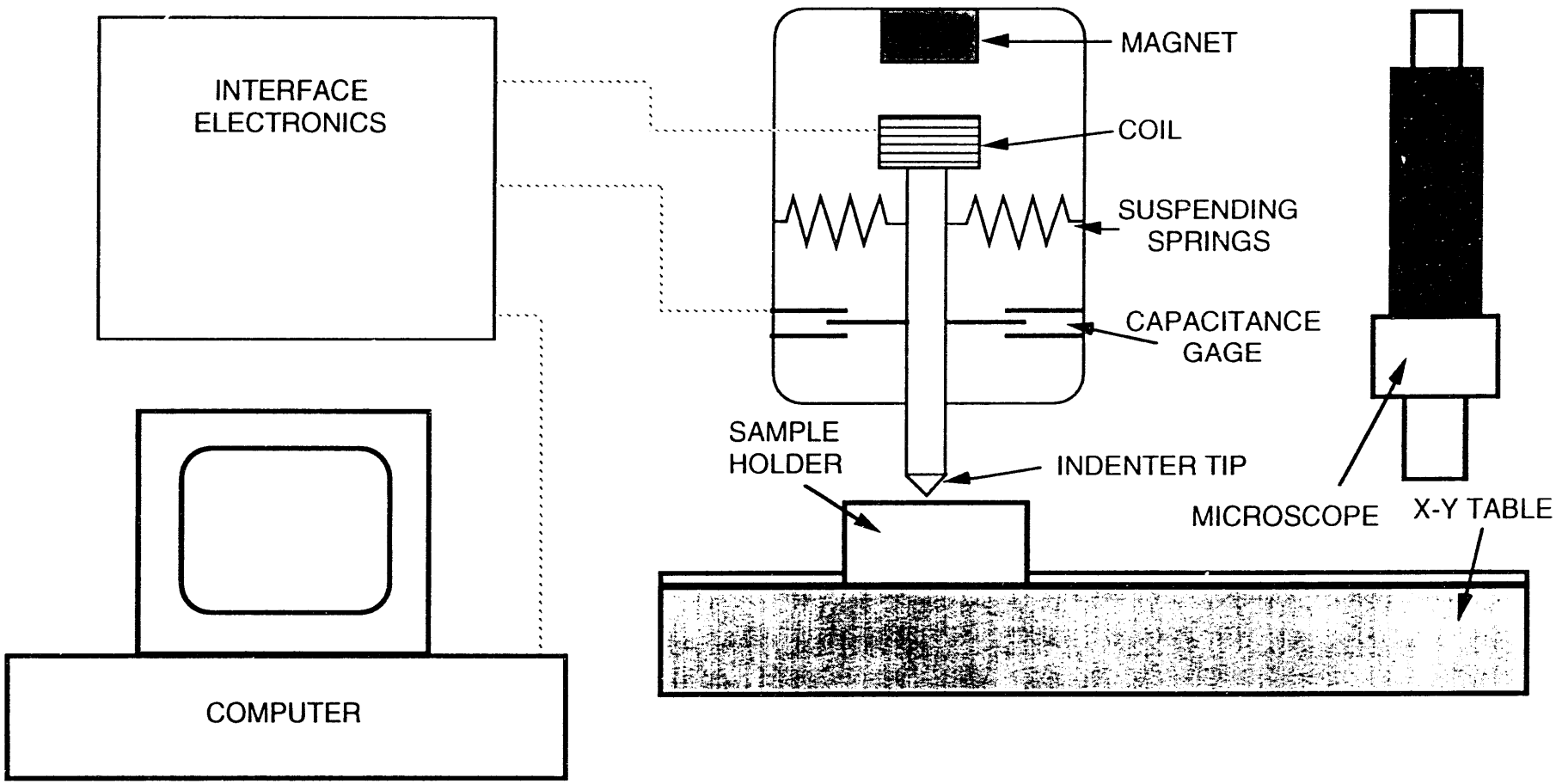

SLIDING DISPLACEMENT FOR A FIBER LOADED WITH THE NANOINDENTER IS OBTAINED BY SUBTRACTING THE INDENTER PENETRATION DISPLACEMENT FROM THE TOTAL DISPLACEMENT

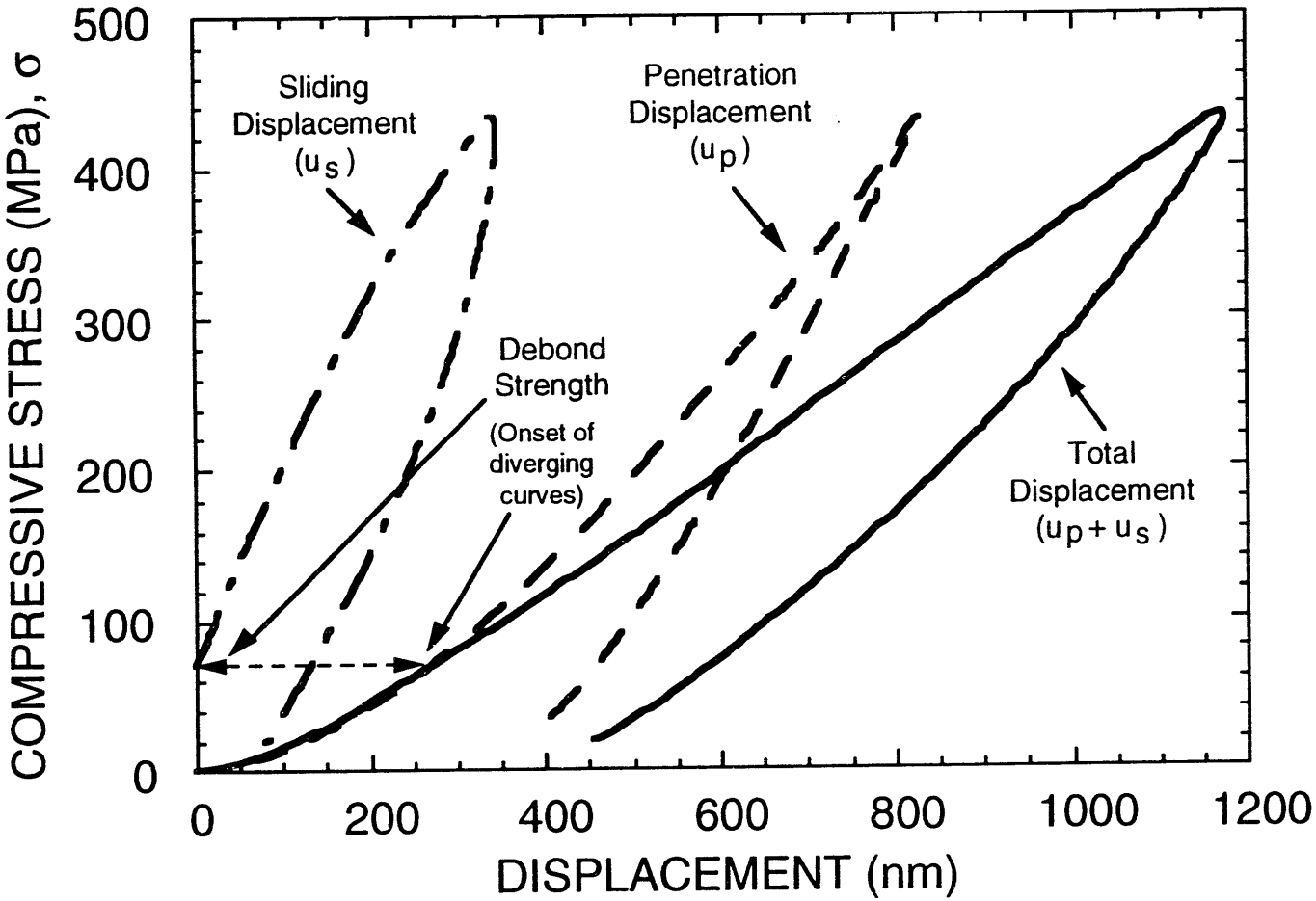

SEVERAL INTERFACIAL PROPERTIES ARE READILY MEASURED FROM STRESS-DISPLACEMENT CURVES GENERATED DURING FIBER PUSH-IN TESTS

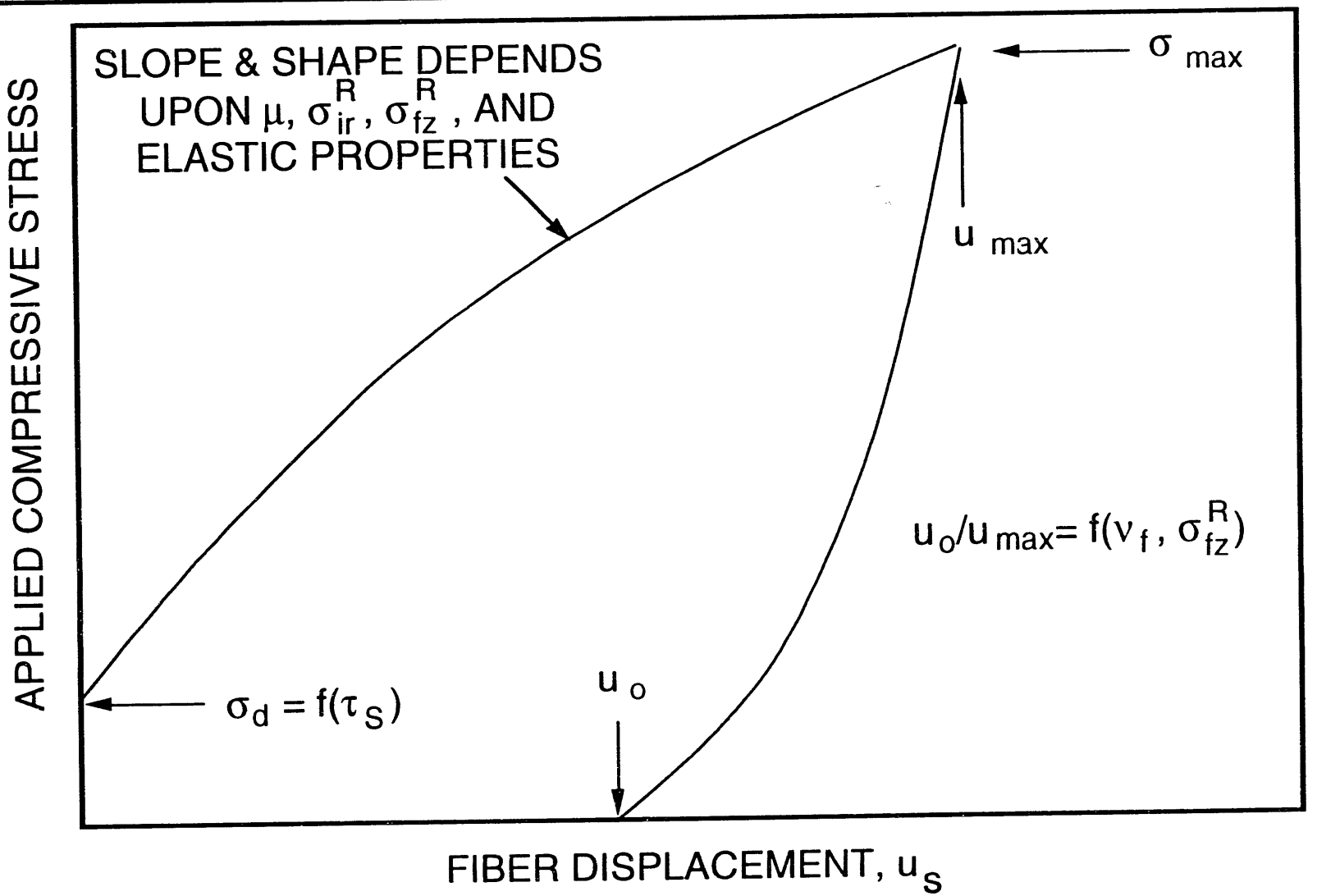

EFFECTIVE CLAMPING STRESS ON THE FIBER DEPENDS ON BOTH THE POISSON'S RATIO OF THE FIBER AND THE RESIDUAL RADIAL STRESS

CONSTANT RADIAL CLAMPING ARISING FROM THERMAL EXPANSION MISMATCH

$$\tau_i = \mu \, (\sigma_{ir}^{R} + \sigma_{ir})$$

RADIAL STRESS GENERATED FROM POISSON'S EXPANSION OR CONTRACTION OF THE FIBER (DECREASES WITH INCREASING DISTANCE BELOW THE SURFACE)

END OF SLIDING ZONE (RESIDUAL AXIAL STRESS IN THE FIBER INFLUENCES BOUNDARY CONDITIONS)

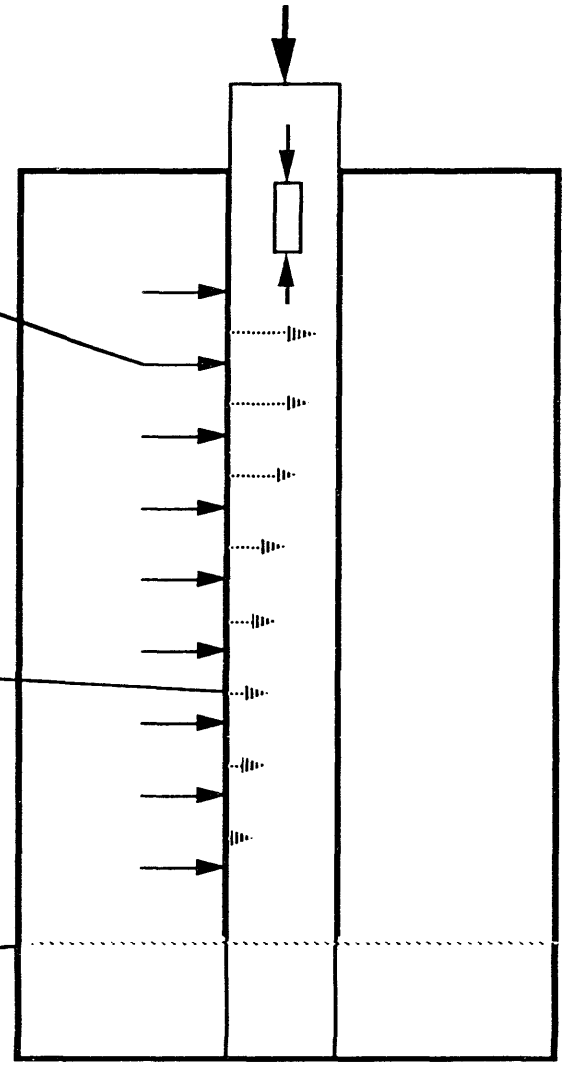

CURRENT PROGRAM ALSO ADDRESSES THE APPLICATION AND VERIFICATION OF STRESS-DISPLACMENT MODELLING EFFORTS MADE BY SEVERAL AUTHORS

- MARSHALL AND OLIVER (1987 AND 1990)
  - BOTH LOADING AND UNLOADING CURVES CONSIDERED
  - MODEL ASSUMES A CONSTANT INTERFACIAL SHEAR STRESS
  - EFFECTS OF RESIDUAL AXIAL STRESS AND DEBONDING ARE INCLUDED IN THE ANALYSIS

- HSUEH (1989-1992)
  - POISSON'S EFFECTS ARE SPECIFICALLY ADDRESSED
  - RADIAL DEPENDENCE OF AXIAL STRESS IN FIBER INCLUDED IN THE SHEAR-LAG ANALYSIS
  - SIMPLIFIED ANALYSIS RECENTLY PROPOSED TO ACCOUNT FOR EFFECTS OF POISSON'S RATIO, DEBOND STRESS, AND RESIDUAL AXIAL STRESS

- KERANS ET AL. (1991)
  - MODEL ACCOUNTS FOR RESIDUAL AXIAL STRESS, POISSON'S RATIO, DEBOND STRESS, AND FIBER SURFACE ROUGHNESS
  - MATRIX STRESSES ARE IGNORED IN THE ANALYSIS
  - MODEL RECENTLY EXTENDED TO UNLOADING

- D. B. MARSHALL (1992)
  - EXTENSION OF THE MODEL BY HUTCHINSON AND JENSON

DIFFERENCES IN MODEL PREDICTIONS CAN BE ATTRIBUTED TO POISSON'S RATIO EFFECTS

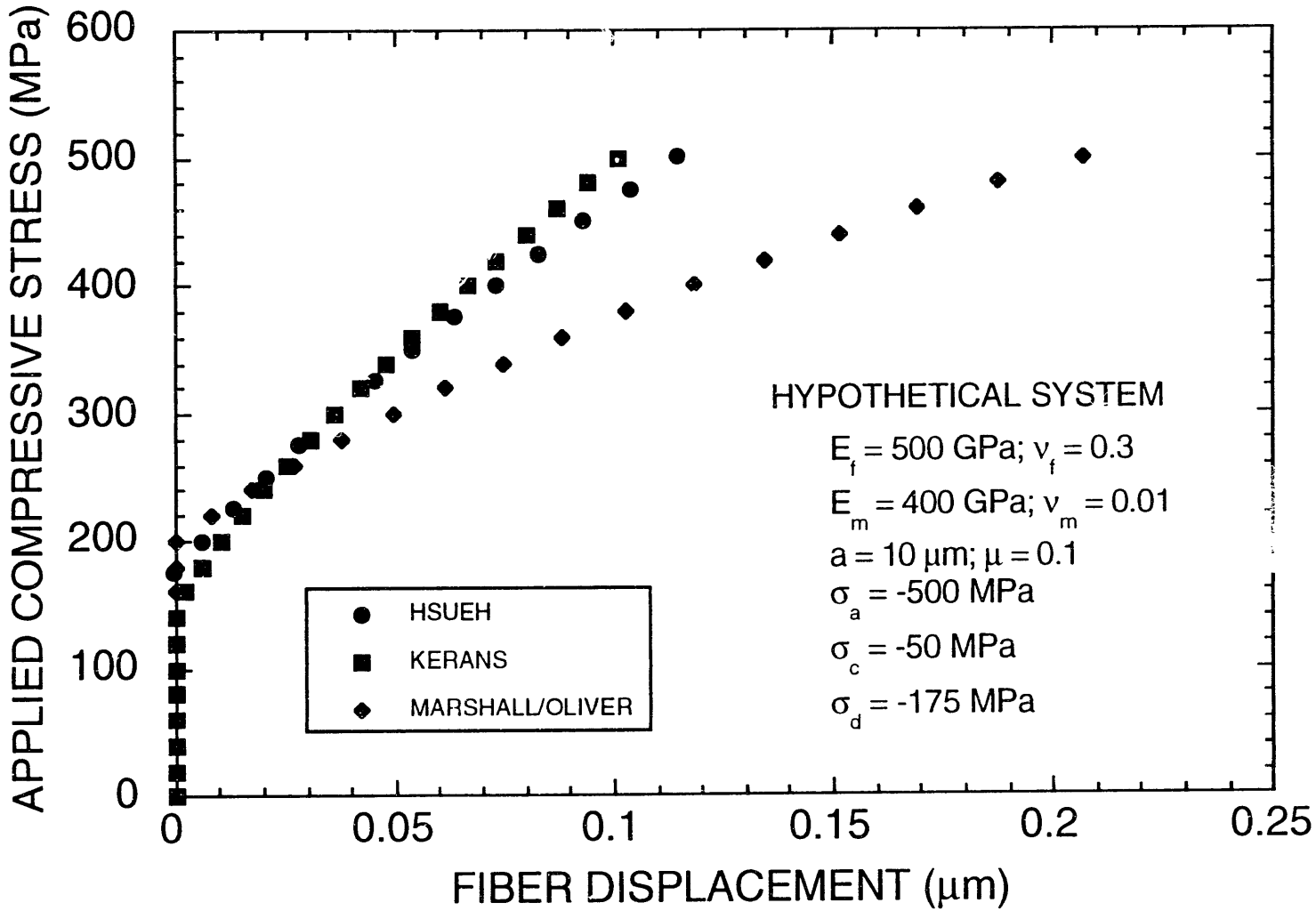

A NUMBER OF EXPERIMENTAL COMPOSITE SYSTEMS HAVE BEEN EXAMINED TO DATE

- NICALON SiC FIBERS IN A LAS GLASS MATRIX
  - EFFECT OF PROCESSING UPON INTERFACIAL PROPERTIES EXAMINED
- NICALON SiC FIBERS IN A MACRO-DEFECT-FREE CEMENT MATRIX
  - EFFECT OF FIBER TREATMENTS UPON INTERFACIAL PROPERTIES EXAMINED
- NICALON SiC FIBERS IN A CVI SiC MATRIX
  - INTERFACIAL PROPERTIES EVALUATED AS A FUNCTION OF FIBER COATING THICKNESS
- MULLITE FIBERS (NEXTEL 480) IN A GLASS MATRIX
  - INTERFACIAL PROPERTIES EVALUATED FOR BN COATED AND UNCOATED FIBERS

EARLY RESULTS FOR NICALON SiC FIBER-REINFORCED LAS GLASS ILLUSTRATE THE IMPORTANCE OF POISSON'S EXPANSION OF THE FIBER DURING INDENTATION LOADING AND UNLOADING

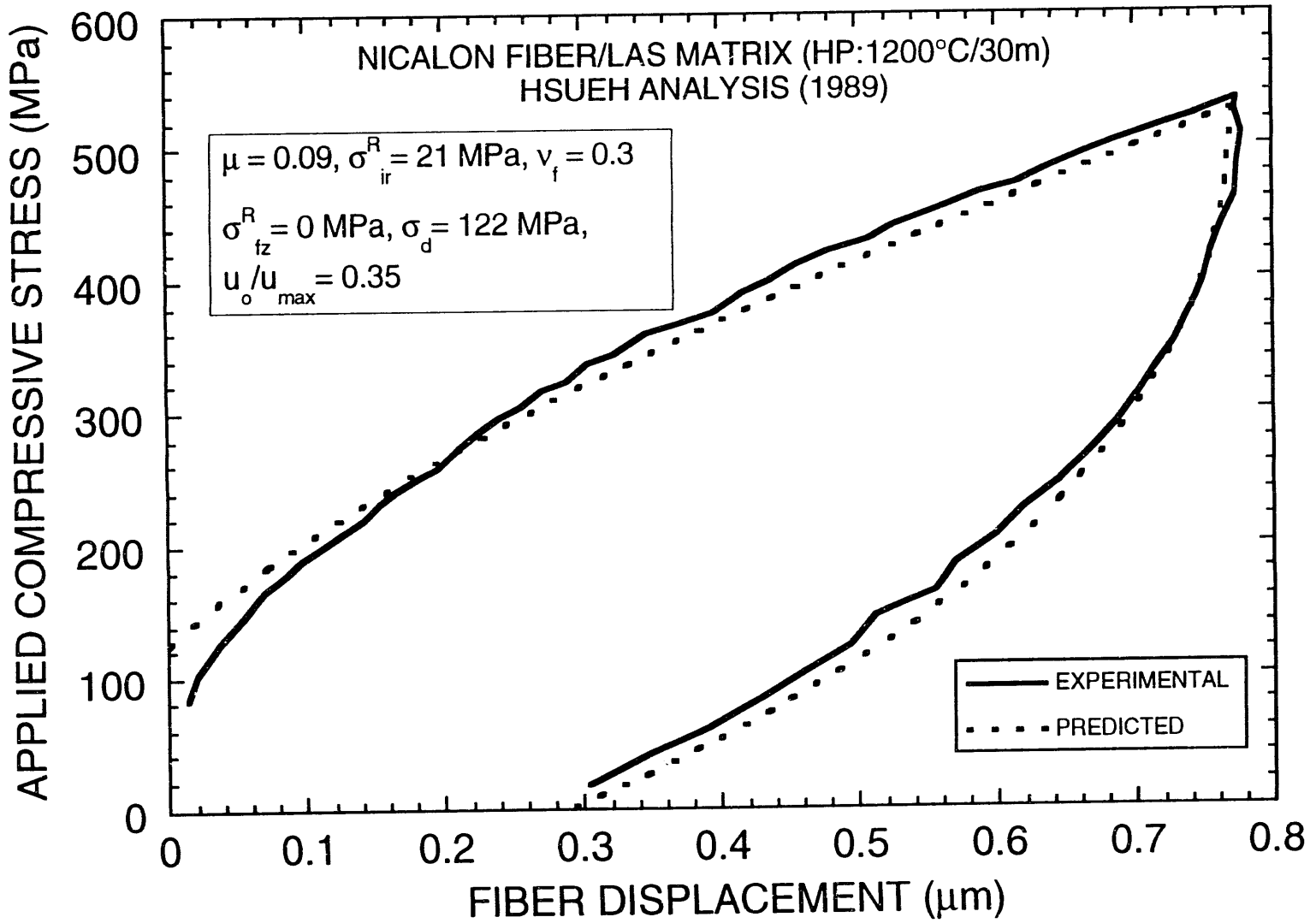

COMPETING EFFECTS OF POISSON'S RATIO AND RESIDUAL AXIAL STRESS HAVE RECENTLY BEEN DEMONSTRATED FOR NICALON SiC FIBER-REINFORCED LAS GLASS

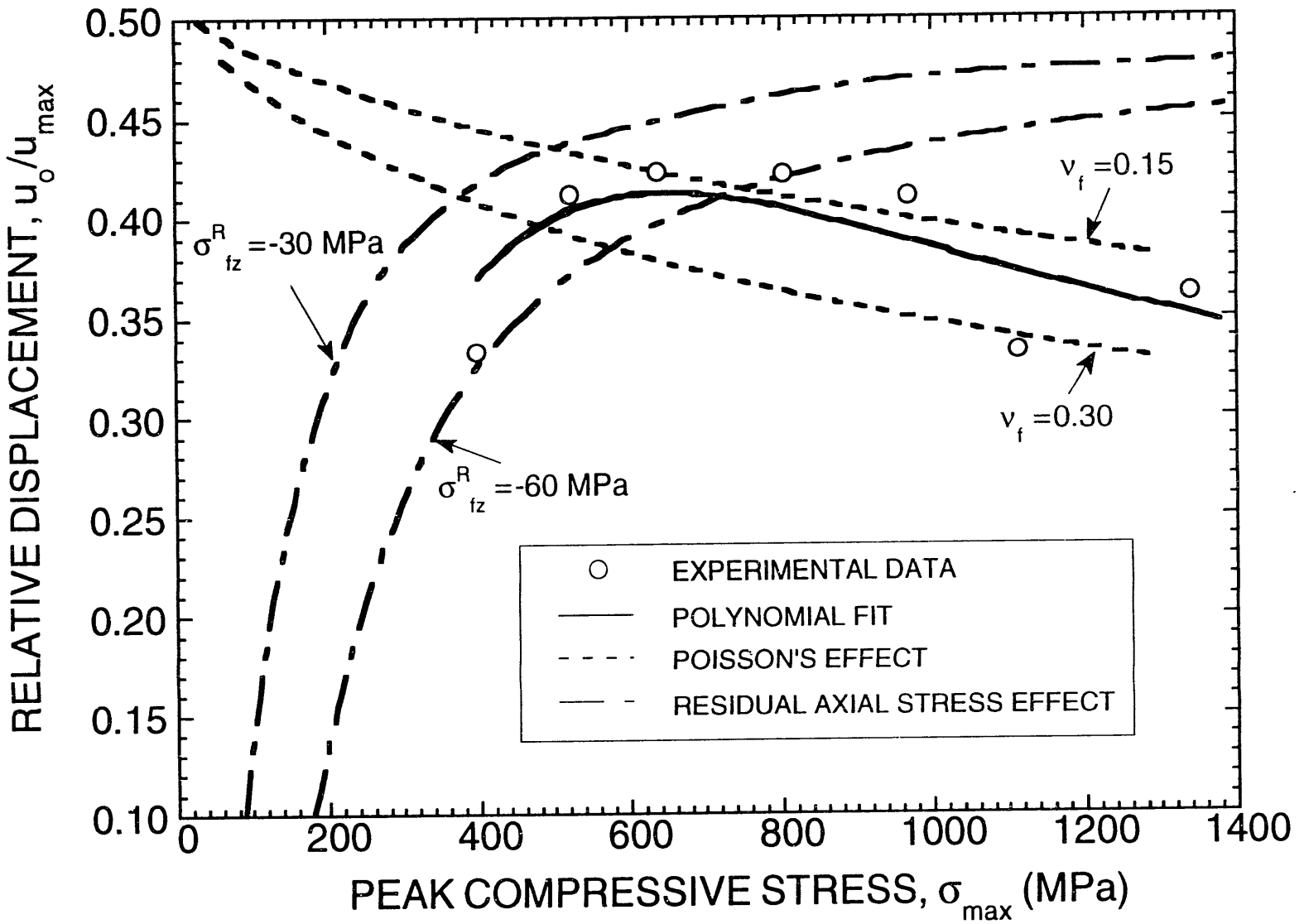

FIBER SLIDING CHARACTERISTICS OF NICALON SiC FIBER-REINFORCED MDF CEMENT ARE STRONGLY INFLUENCED BY FIBER TREATMENTS

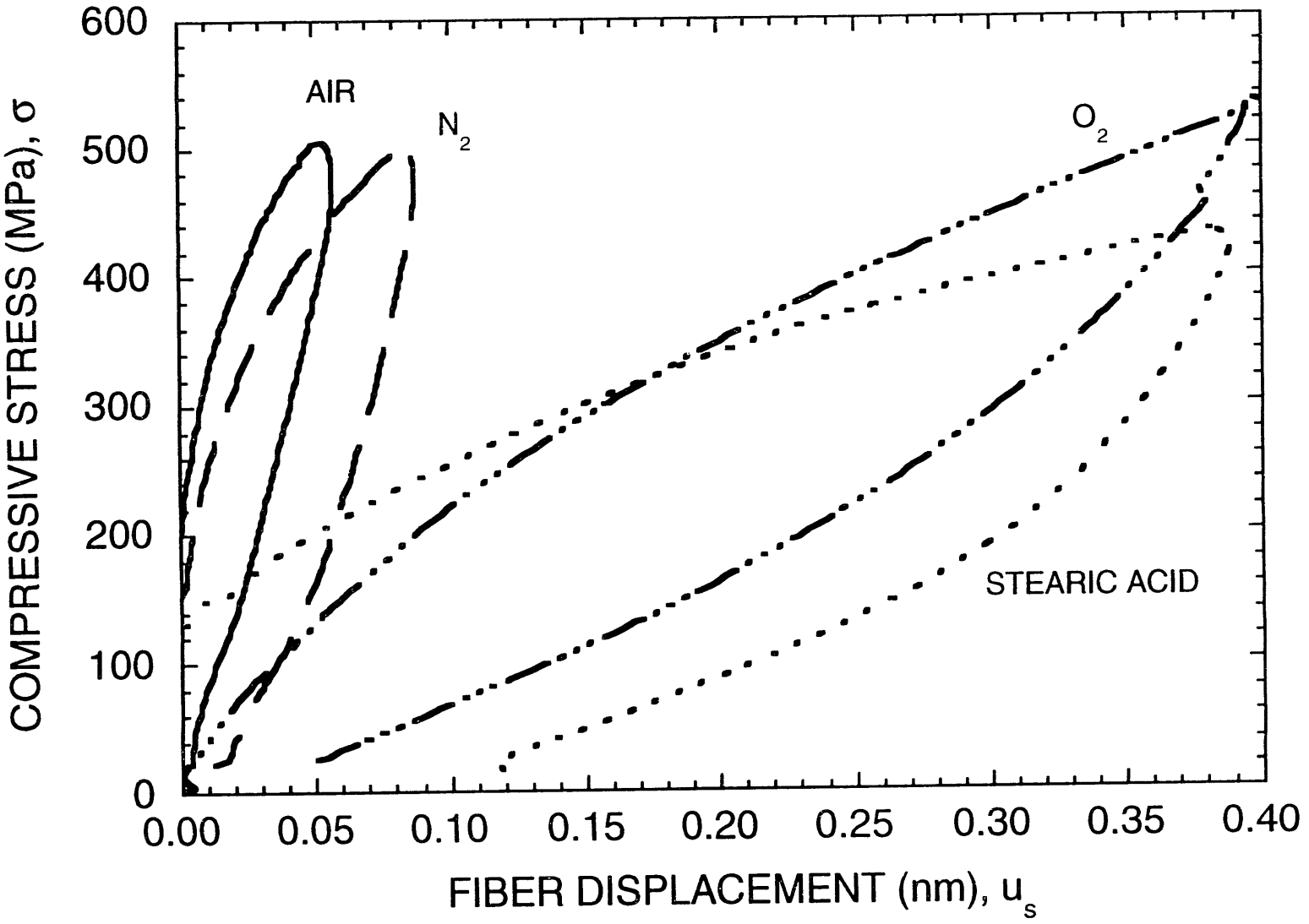

RESIDUAL AXIAL STRESSES PLAY A SIGNIFICANT ROLE IN THE FIBER SLIDING CHARACTERISTICS OF NICALON SiC FIBER-REINFORCED MDF CEMENT

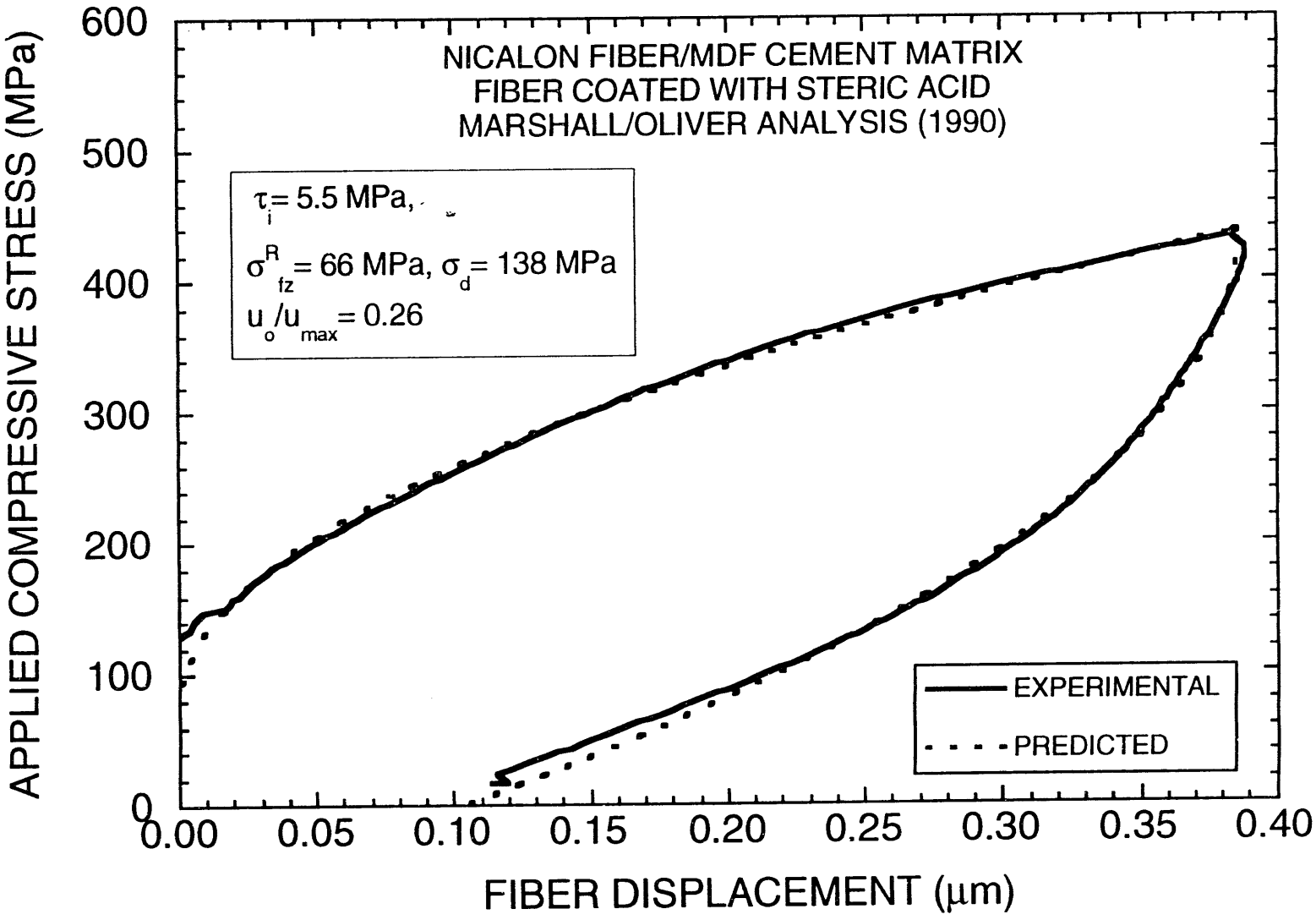

FIBER RECOVERIES EXCEEDING INITIAL FIBER POSITION HAVE ALSO BEEN MEASURED FOR NICALON SiC FIBER-REINFORCED MDF CEMENT

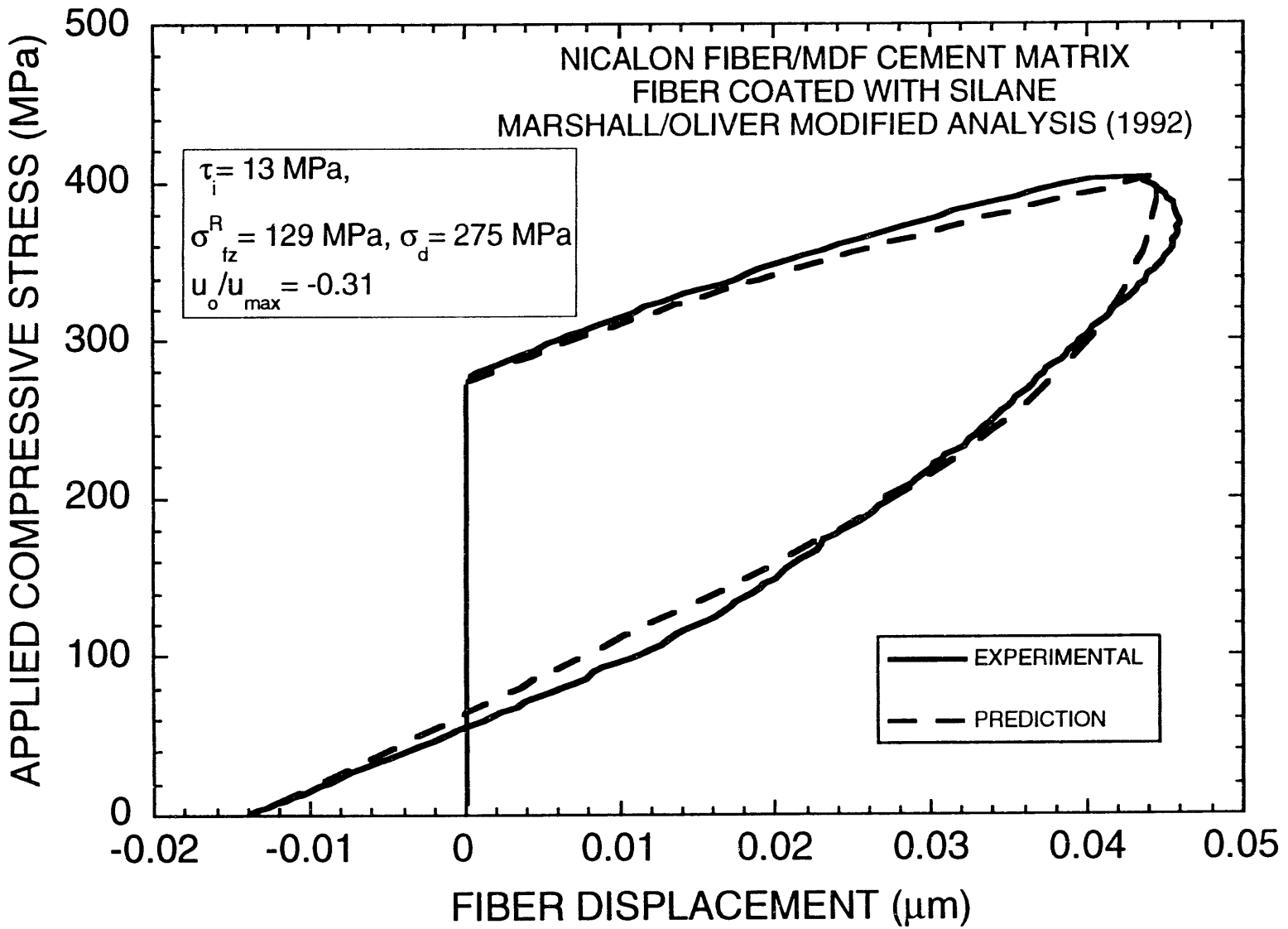

RESIDUAL AXIAL STRESS EFFECTS DOMINATE FIBER RECOVERY IN NICALON SiC FIBER-REINFORCED MDF CEMENT

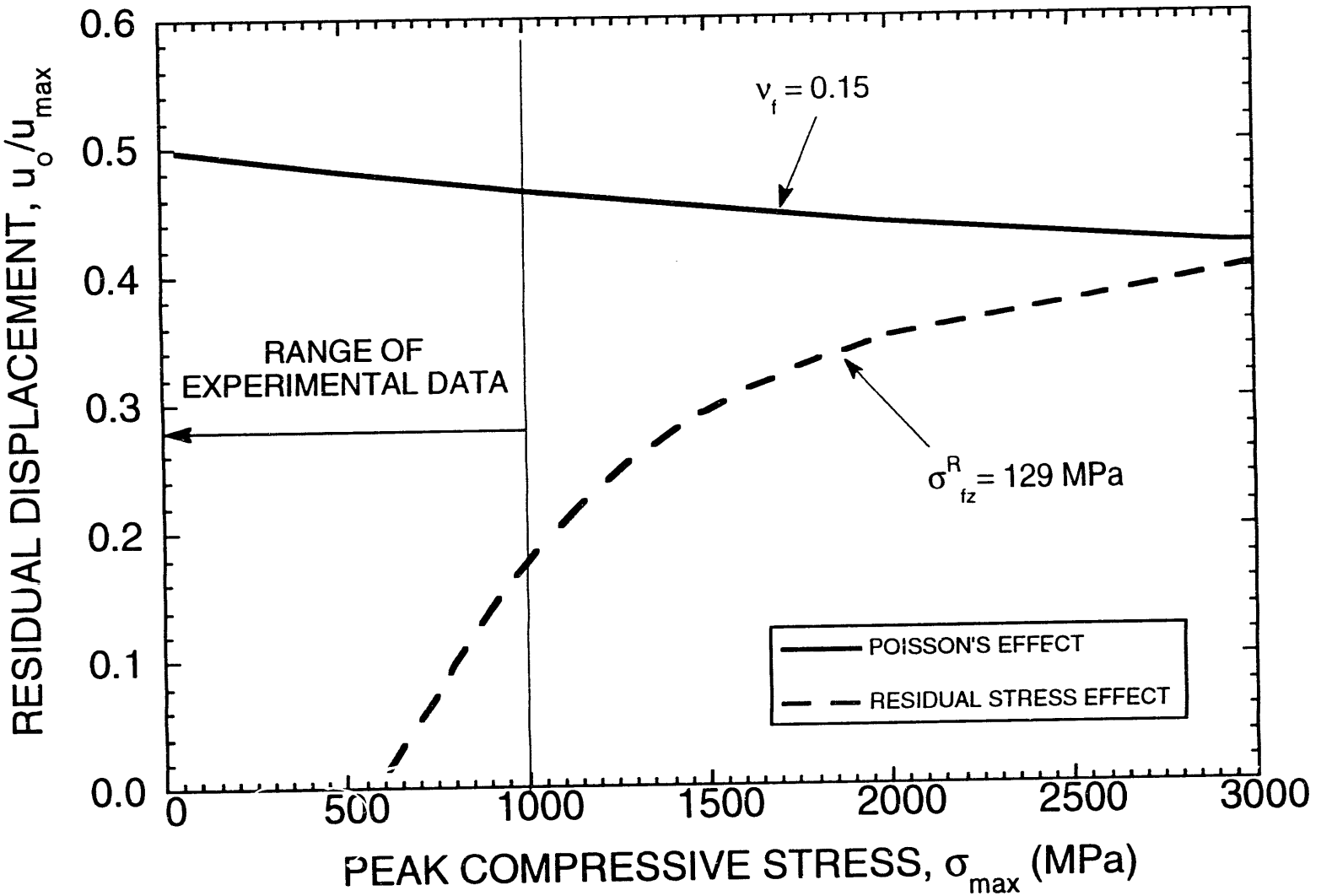

OXIDE SYSTEMS STUDIED TO DATE HAVE EXHIBITED LIMITED SLIDING

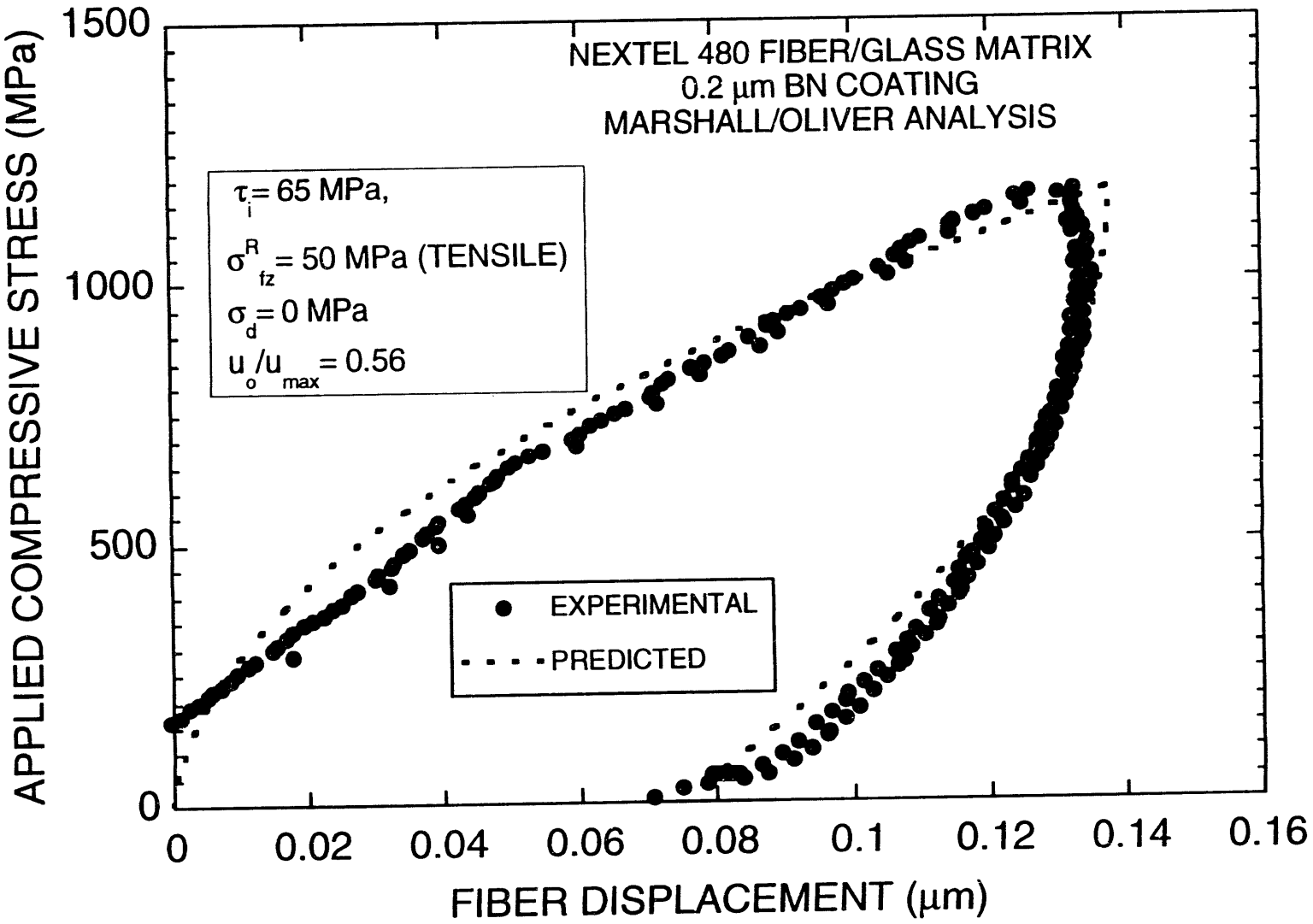

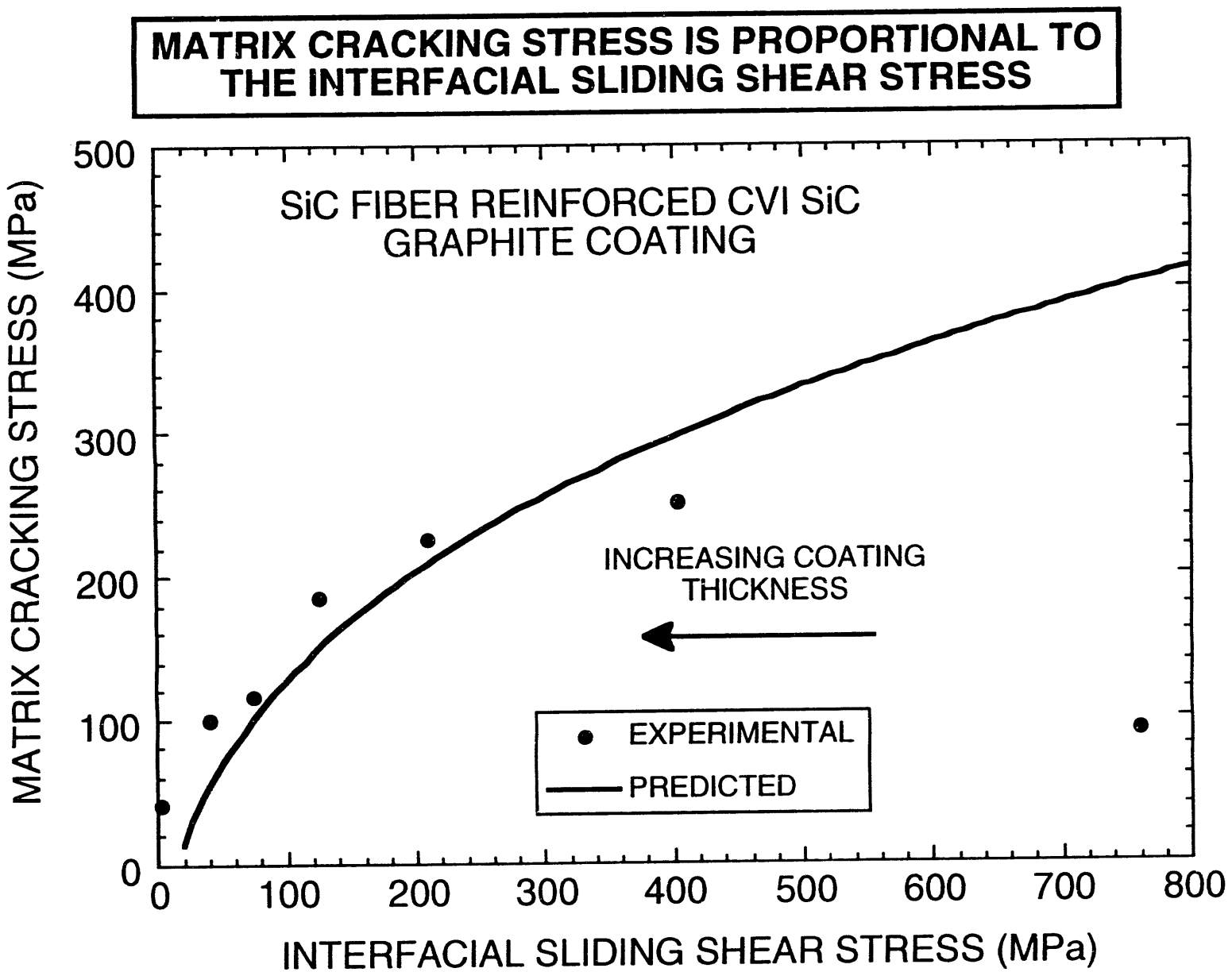
MATRIX CRACKING STRESS IS PROPORTIONAL TO THE INTERFACIAL SLIDING SHEAR STRESS
SiC FIBER REINFORCED CVI SiC GRAPHITE COATING
INCREASING COATING THICKNESS
EXPERIMENTAL
PREDICTED
MATRIX CRACKING STRESS (MPa)
INTERFACIAL SLIDING SHEAR STRESS (MPa)
0
100
200
300
400
500
600
700
800

MAGNITUDE OF THE RESIDUAL AXIAL MATRIX STRESSES HAS BEEN FOUND TO BE A CRITICAL FACTOR IN DETERMINING THE MATRIX CRACKING STRESSES

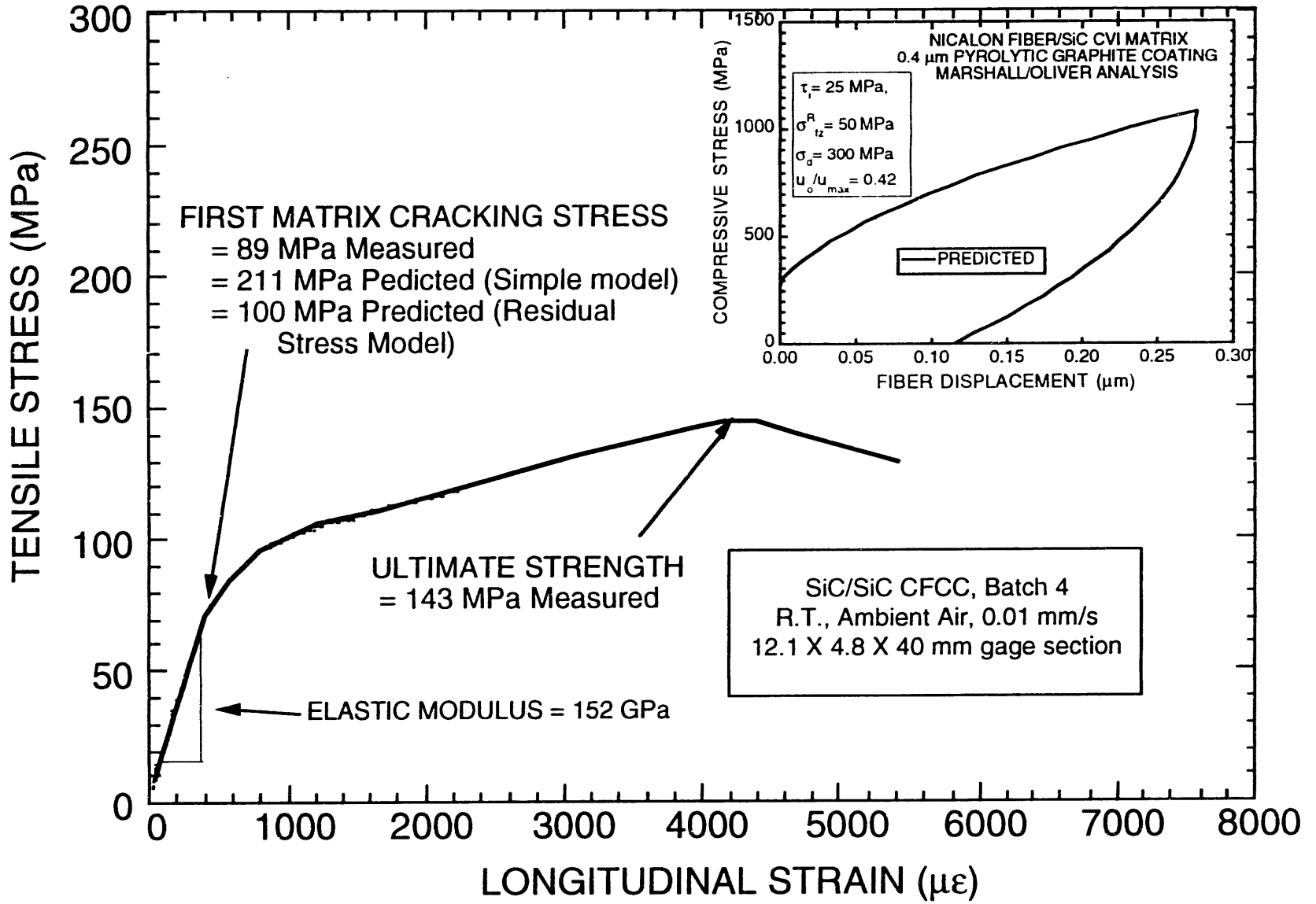

CONCLUSIONS

- PUSH-IN STUDIES UTILIZING THE NANOINDENTER ARE MOST PROMISING FOR SMALL FIBERS WITH LOW VALUES OF THE INTERFACIAL SLIDING SHEAR AND DEBOND STRESSES
  - EXAMINATION OF LARGER FIBERS WILL REQUIRE HIGHER CAPABILITY

- BOTH POISSON'S RATIO AND RESIDUAL AXIAL STRESS CAN HAVE A SIGNIFICANT INFLUENCE ON INTERFACIAL PROPERTIES
  - RELATIVE FIBER RECOVERY IS A PRIMARY INDICATOR OF RESIDUAL AXIAL STRESS

- PREDICTED VALUES OF FIRST MATRIX CRACKING BASED ON INTERFACIAL PROPERTIES ARE IN REASONABLE AGREEMENT WITH EXPERIMENTAL MEASUREMENTS

- MODEL DEVELOPMENT IN SEVERAL AREAS IS REQUIRED FOR ANALYSIS OF REAL COMPOSITE SYSTEMS
  - COMPLICATED FIBER ARCHITECTURES
  - ANISOTROPY OF ELASTIC PROPERTIES
  - THREE COMPONENT SYSTEMS (FIBER/COATING/MATRIX)

UTILITY OF EXISTING MODELS IS LIMITED BY SEVERAL FACTORS

- NO MODEL ADEQUATELY ACCOUNTS FOR EFFECTS OF DEBONDING, POISSON'S EXPANSION/CONTRACTION, OR RESIDUAL AXIAL STRESS
  - UNDERLYING MODEL ASSUMPTIONS MUST ALSO BE EXAMINED
- CURRENT MODELS ARE RESTRICTED TO TWO-COMPONENT SYSTEMS
  - INTERFACIAL FILM WILL COMPLICATE THE SHEAR TRANSFER PROCESS
  - INITIAL RESIDUAL STRESS STATE IS MORE COMPLEX WHEN A COATING IS PRESENT
- ELASTIC PROPERTIES OF THE FIBER, MATRIX, AND COATING ARE ASSUMED TO BE ISOTROPIC
  - COATING ANISOTROPY IS EXPECTED TO SIGNIFICANTLY INFLUENCE THE TRANSVERSE PROPERTIES

ONGOING MODELLING EFFORTS ARE FOCUSED ON THE FIRST TWO ITEMS

DATE FILMED

8/17/93

END